CHARACTERIZATION OF PERMANENT FOULING ON THE SURFACES OF UV LAMPS USED FOR DISINFECTION

by

Ji Peng

Department of Civil Engineering and Applied Mechanics
McGill University
Montreal, Canada

November, 2002

A thesis submitted to McGill University in partial fulfilment of the requirements for the degree of Master of Engineering

Your file Votre référence
ISBN: 0-612-88380-9
Our file Notre référence
ISBN: 0-612-88380-9

Abstract

A significant problem with UV disinfection is the accumulation of inorganic and organic fouling materials at sleeve-water interfaces. Fouling necessitates the need for cleaning of quartz sleeves to maintain optimal system efficiency and performance. It has been shown that chemical/mechanical cleaning can remove fouling materials satisfactorily. However, there are always permanent foulants, which cannot be removed completely by normal cleaning operations, remaining on quartz sleeves. These permanent foulants will weaken UV transmittance, in turn reducing disinfecting effectiveness.

This research investigated the origins and formations of permanent fouling. Four instrumental analyses were employed. They were Sleeve UV Transmittance (SUVT), Atomic Force Microscope (AFM), X-Ray Fluorescence (XRF), and Scanning Electron Microscope (SEM) combined with Energy Dispersive X-ray Microanalysis (EDX).

It was verified that permanent foulants were trapped initially by the inherent holes and peaks on sleeve surfaces. After long term periodical chemical/mechanical cleaning, the wipers of cleaning systems would damage sleeve surfaces severely, causing scratches or holes with wide surface areas, which may be termed mechanical deterioration of the sleeves. Thus, foulants would be trapped more easily by these scratches, and would be attached tightly to the surfaces of these scratches or to each other. Using instrumental analyses, the compositions of permanent foulants were found to be site specific. In general, iron, aluminum, calcium, magnesium and phosphorus composed the majority of the components of the permanent foulants.

Since mechanical damage cannot be avoided altogether because it is induced by the cleaning systems, the practical way for reducing the effect of permanent foulants is to choose the most suitable cleaning chemicals. Sodium hydroxide, sodium bisulfite and phosphoric acid appeared to be suitable agents.

This research attempted to correlate permanent fouling to the site-specific wastewater quality. However, although it seemed that wastewater quality could affect permanent fouling to some extent, there was no robust relationship between them. Thus, wastewater quality parameters cannot be used at this stage to predict the future influence of that wastewater on permanent fouling.

Résumé

Un problème significatif avec la désinfection UV est l'accumulation des matériaux d'encrassement inorganiques et organiques aux interfaces de l'eau et du manchon. Un nettoyage approfondi des manchons de quartz est nécessaire afin de maintenir une efficacité optimal du systeme. Il a été demontré que le nettoyage chimico-mécanique peut désencrasser d'une manière satisfaisante. Cependant il reste toujours des résidus permanents pour lesquels un nettoyage normal est insuffisant sur les manchons de quartz. Ces minuscules impuretés restantes affectent la transmission des UV réduisant ainsi l'efficacité du systeme.

Cette recherche a étudié l'origine et la formation de l'encrassement permanent a l'aide de quatre analyses instrumentales : la transmittance UV de douille, le microscope atomique de force, la fluorescence de rayon X, et le microscope électronique combiné avec la microanalyse dispersive de rayons X d'énergie.

Les résidus permanents sont au début emprisonnés par les trous et les cretes de la surface du manchon. A long terme, les nettoyages chimico-mecaniques endommageraient sevèrement les surfaces du manchon entrainant des éraflures et des trous aux dimensions sinificatives que l'on peut dénomer déterioration mécanique des manchons. Ainsi les résidus seraient emprisonnés encore plus facilement par ces éraflures, accrochés aux surfaces des éraflures ou entre eux. En utilisant des analyses instrumentales, les compositions des residus permanents se sont révélés d'être spécifique selon les caractéristiques de chaque emplacement. En général, le fer, l'aluminium, le calcium, le magnésium et le phosphore constituent la majorité de composants des residus permanents.

Puisque des dommages mécaniques ne peuvent pas être évités tout à fait parce qu'ils sont induits par les systèmes de nettoyage, la manière pratique pour réduire l'effet des residus permanents est de choisir les produits chimiques de nettoyage les plus appropriés.

L'hydroxyde de sodium, le bisulfite de sodium et l'acide phosphorique ont semblé convenir les agents.

Cette recherche a essayé de trouver une corrélation entre l'encrassement permanent et la qualité des eaux usées. Cependant bien que la qualité des eaux usées pourrait dans une certaine mesure affecter l'encrassement permanent il n'y aurait qu'un rapport robuste entre eux. Ainsi les paramètres des eaux usées ne peuvent pas être employés pour prévoir la future influence de ces eaux sur l'encrassement permanent. Ainsi, des paramètres de qualité d'eau usée ne peuvent pas être employés à ce stade pour prévoir la future influence de cette eau usée sur l'encrassement permanent.

Acknowledgements

I would like to thank my supervisor Professor Ronald Gehr, whose valuable advice and guidance helped me greatly throughout my research period.

I would also like to extend my appreciation to Ms. Daina Brumelis, Mr. Lang Shi, Mr. Tariq Ahmedali, Ms. Glenna Keating and Ms. Helen Campbell, for their patience and assistance.

Special gratitude to Mr. Mike Oliver and Mr. Yannick Vinette, for their cooperation and generosity in supplying samples.

I am grateful to all the members of Ultraviolet Disinfection Research Group in the Department of Civil Engineering & Applied Mechanics at McGill University for their ideas and friendship.

Deepest gratitude to my mother, my father, and my sisters, for their encouragement and invaluable love.

Table of Contents

List of Figures

List of Tables

Chapter 1 Introduction

Ultraviolet (UV) disinfection is employed as the main alternative to chemical disinfection in wastewater treatment. This process is simple to operate. It achieves disinfection by damaging the microorganism's ability to replicate its DNA (Angehrn, 1984; Bolton, 1999). There are no known toxic by-products (WEF, 1996). A UV disinfection system can work well over a wide range of liquid temperatures (Angehrn, 1984; USEPA, 1986; WEF, 1996). Other advantages of UV disinfection are (Ohio Pure Water Company, 2002):

- Environmentally and user friendly, no dangerous chemicals to handle or store, no risks of overdosing.

- Low initial capital cost as well as reduced operating expenses when compared with similar technologies such as ozone, chlorine, etc.

- On-line treatment process, no need for holding tanks, long retention times, etc.

- No change in taste, odour, pH or conductivity nor the general chemistry of the water.

- Compatible with all other wastewater treatment processes.

Commonly used low or medium pressure mercury arc lamps generating UV radiation at wavelengths around 253.7 nm are used for the radiation sources. The lamps are housed in quartz sleeves to permit immersion in the aqueous stream being subjected to irradiation. If the quartz sleeves are clean enough, sufficient UV energy will pass through the sleeves, killing microorganisms in the wastewater effectively. Thus, it can be concluded that the efficiency of UV disinfection is strongly affected by the UV transmittance of the quartz sleeves.

A significant problem with UV disinfection is the accumulation of inorganic and organic fouling materials at the sleeve-water interfaces. These fouling materials absorb UV radiation, therefore decreasing the intensity of UV light penetration into the wastewater (Blatchley et al., 1996). The mechanism of the fouling process is complicated, so the fouling process is site specific and often difficult to predict. The fouling process is hypothesised to be attributable to physicochemical processes occurring in the aqueous phase immediately adjacent to the sleeve-water interface (Lin, 2000).

Factors such as interfacial temperature, UV intensity, hydrodynamics, the sleeve microstructure and topography, wastewater composition and flow rate can influence the fouling process (Lin et al., 1999b; Sheriff and Gehr, 2001). In the fouling materials, iron, aluminium and calcium were found to represent the majority of cations; and carbonate, sulfate, chloride and phosphate were the predominant anions (Blatchley et al., 1996; Lin et al., 1999a). When metal salts, such as iron or aluminium, are added to the wastewater for coagulation and flocculation, they will aggravate the fouling (Lin et al., 1999a; Sheriff and Gehr, 2001). Recent research has also shown that the fouling process was dependent on the cleaning methods (Qiu, 2001; Oliver, 2002).

Fouling necessitates the need for cleaning of the quartz sleeves to maintain optimal system efficiency and performance. Since wastewater treatment plants vary in both scale and wastewater quality, unique methods of cleaning are devised for individual systems. The normal cleaning methods can be divided into chemical/mechanical cleaning and mechanical cleaning. Mild detergents can be used for chemical/mechanical cleaning. Phosphoric acid of pH 1-2 is also a recommended cleaning chemical (WEF, 1996; Oliver, 2002). Frequency of cleaning is a function of the flow capacity and the treatment prior to disinfection.

When studying the permanent fouling of the quartz sleeves (i.e. foulant which could not be removed by normal cleaning operations), the fouling was found to be a function of time (Qiu, 2001). Direct ion exchange on the quartz surface played only a minor role in the accumulation of metals on quartz surfaces. Precipitation played a dominant role in quartz surface fouling. When the UV lamp was off, organic fouling dominated; this could be removed by switching on the lamp. Thus, organic fouling was not a serious (permanent fouling) problem. Inorganic accumulation was found to be promoted by UV radiation.

Some experiments have shown that chemical/mechanical cleaning can remove the fouling materials satisfactorily (Qiu, 2001; Oliver, 2002). However, the quartz samples used in these experiments only experienced a short-term operation (less than 6 months), and wastewater quality was not taken into account. Therefore, there is little information regarding the correlation between wastewater quality and permanent fouling. Furthermore, a quantitative analysis of the chemical components of permanent fouling, which will verify if the permanent fouling on the sleeves from different wastewater plants has a similar composition, has not been done systematically.

Thus the objectives of this study are to analyze the extent of deterioration of the quartz sleeves surrounding UV lamps after a long-term application and frequent cleaning, which may be crucial to the presence of permanent fouling. It also attempts to validate a relationship between the mode of cleaning, as well as wastewater quality, and the extent of permanent fouling. The analysis was performed using the following techniques:

- Sleeve UV Transmittance Test (SUVT)
- Atomic Force Microscope (AFM)
- X-Ray Fluorescence (XRF)
- Scanning Electron Microscope (SEM) combined with Energy Dispersive X-ray Microanalysis (EDX).

Chapter 2 Literature Review

2.1 UV Disinfection

UV disinfection uses short-wave UV light to inactivate pathogens. Wastewater flows through or around a tube with UV light penetrating it from all directions. The UV light disrupts the DNA strands of the microorganisms in the wastewater and prevents them from replicating. UV disinfection requires a minimum applied dosage ("fluence") to be effective. This applied fluence is a function of the lamp intensity and the exposure time. These parameters are directly affected by equipment configuration, flow path of the wastewater through the bank of lamps, plus the solids content and the UV transmittance of the wastewater to be disinfected (USEPA, 2002). The effectiveness of a UV disinfection system depends on the characteristics of the wastewater, the intensity of UV radiation, the time the microorganisms are exposed to the radiation, and the reactor configuration.

UV disinfection has several advantages over conventional chemical disinfection including generally lower effluent toxicity (Blatchley et al., 1996), improved operator and community safety, excellent virucidal capacity, and simple operation. Table 2-1 compares UV disinfection to other common methods of disinfection. The disadvantage is that turbidity and suspended solids (SS) in the wastewater can render UV disinfection ineffective because particles in the wastewater will absorb or scatter UV radiation. UV disinfection with low-pressure lamps is not very effective for secondary effluents with SS levels above 30 mg/L (Job et al., 1995; Mishalani et al., 1996; USEPA, 2002). Other factors, such as hardness and pH of the wastewater, can also affect UV disinfection. The poorer the wastewater quality, the lower the disinfection efficacy (Correia and Snider, 1993).

Table 2-1 Comparison between UV disinfection and other methods (Source: Aquionics Inc., 2002)

	Ultra Violet	Chlorine	Ozone
Capital Cost	Low	Lowest	High
Operating Cost	Lowest	Low	High
Ease of Installation	Excellent	Good	Poor
Ease of Maintenance	Excellent	Good	Poor
Cost of Maintenance	Lowest	Medium	High
Frequency of Maintenance	Infrequent	Frequent	Continuous
Control System	Excellent	Poor	Good
Disenfection Performance	Excellent	Leaves some pathogens	Excellent
Hazards	Low	High	High
Effect on water	None	Organochlorine compounds, taste, pH changes	[illegible]
Contact time	0.5-5 seconds	30-60 minutes	10-20 minutes

The source of UV radiation is either low-pressure or medium-pressure mercury arc lamps with low or high UV intensities. Low-pressure lamp systems are suitable for low flow treatment plants. Medium pressure lamp systems are generally suitable for larger flows (Cairns, 1996; O'Brien et al., 1996):

- where space is limited,
- where a reduction in lamp numbers is necessary,
- where facilities for installation of a large number of low pressure lamps is expensive,
- where rapid fouling rates would require very high maintenance expenses

Medium pressure lamps have approximately 15 to 20 times the germicidal UV intensity of low-pressure lamps. The medium pressure lamp disinfects faster and has greater penetration capability because of its higher intensity. However, these lamps operate at higher temperatures with higher energy consumption (USEPA, 2002).

2.2 Fouling

The accumulation of unwanted organic and inorganic deposits on the sleeve-water interfaces of quartz sleeves in UV disinfection systems is referred to as fouling. The foulants absorb UV radiation, thereby inhibiting the potential irradiation of microorganisms in wastewater (Bott, 1995; Blatchley et al., 1996), in turn weakening the efficacy of UV disinfection.

Fouling is a common problem in UV disinfection systems, but the fouling process is site specific and difficult to predict (Job et al., 1995). The rate of fouling is highly variable from site to site, but eventually all sites accumulate foulants at intervals appropriate to the fouling rate (Oliver, 2002). In general, there are three continuous stages of fouling, which may be observed in relation to deposition on the sleeve surface (Stumm, 1992; Bott, 1995):

1. Diffusion transport of the foulant or its precursors across the boundary layers adjacent to the sleeve surface within the flowing wastewater;
2. Adhesion of the deposit to the sleeve surface and to itself;
3. Transport of materials away from the sleeve surface.

2.2.1 Fouling Mechanism

The fouling process is hypothesized to be attributable to physicochemical processes occurring in the aqueous phase immediately adjacent to the sleeve-water interface (Lin, 2000). Although the mechanism of the fouling process is complicated, it has been clear that the direct ion exchange on the quartz surface played only a minor role in the accumulation of metals on quartz surfaces. The photochemical reactions of constituents in the wastewater, which cause colloidal particles to form and settle on sleeves after absorption of UV energy, are considered as another contributor (Lin et al., 1999a). However, the accepted dominant mechanism in fouling is precipitation and flocculation (Bott, 1995; Diamant, 1996; Lin, 2000; Sheriff and Gehr, 2001).

Bott (1995) and Muller (2000) divided fouling mechanisms into five major categories according to the key physical/chemical processes involved:

- Crystallisation fouling

This is the precipitation and deposition of dissolved inorganic salts, which at process conditions become supersaturated at the sleeve-water surface. Supersaturation may be caused by: (1) the heat released from the UV lamps, resulting in a local warming of wastewater near the sleeve-water surface. Since many metals in wastewater have inverse solubility (the solubility decreases with temperature increment), they may crystallize and precipitate on the sleeve surface (Lin, 2000). (2) pH and hardness changes, which can change the solubility of metals and metal-ligand compounds in the wastewater, thus leading to deposition (USEPA, 2002).

- Particulate fouling

Small suspended particles, such as sand, clay, and chemical products, will deposit on the sleeves by gravitational settling, Brownian motion, or interception. This type of fouling is likely to occur with wastewaters after the addition of aluminum or iron salts for coagulation, which will contain considerable numbers of particles.

- Chemical reaction fouling

Foulants are formed on the surface of sleeves as the result of chemical reactions in which the surface material itself does not participate.

- Corrosion fouling

Corrosion fouling may be regarded as reaction fouling, with the chemical reactions involving the sleeve surface. Corrosion can be defined as the deterioration and loss of material due to some form of chemical attack. The origin of the corrosion may be the wastewater itself, or a constituent in the wastewater. Corrosion is often accelerated by the presence of other deposits such as scale, biofilms, and biota (Bott, 1995). Moreover, the thermal resistance of a corrosion layer is usually low because of the relatively high thermal conductivity of foulants, therefore it may promote fouling associated with other fouling mechanisms.

- Biological fouling

This refers to the development and deposition of organic films consisting of microorganisms and their products, and the attachment and growth of macroorganisms on the sleeve surface. Microbes attach to the sleeve surface, forming biofilms that can scavenge nutrients from the wastewater. The composition of biofilms may be greatly influenced by the type of microbes involved, the composition of wastewater (nutrient source), the temperature, the hydrodynamic conditions, and the mechanical stability of biofilms (Geesey et al., 1993; Gaylarde and Videla, 1995).

Although it has been assumed that these mechanisms may occur concurrently and are jointly responsible for the overall fouling phenomena, it is still important to identify a dominant mechanism or a combination of mechanisms for fouling in a specific UV disinfection system, so that an effective control can be implemented.

2.2.2 Foulant Composition

In the foulant, iron, aluminum and calcium are generally found to represent the majority of cations. According to studies by Blatchley (1997), and Lin et al. (1999a), calcium was observed to be the dominant metal, while iron and aluminum also made substantial contributions, even though they were not at high concentrations in the wastewater. Carbonate, hydroxide, sulfate, chloride and phosphate were the predominant anions.
These cations and anions, which are combined as mixed-ligands, will form various complexing compounds. The high concentrations of DOC (dissolved organic carbon) in wastewater could also increase the complexation of metals composition in the fouling materials (Lin et al., 1997). The presence of these complexing compounds associated with their respective solubility limits will virtually guarantee precipitation. Previous research has shown that a broad spectrum of metals and anionic ligands was present in the fouling materials (Lin et al., 1997), which is compatible with the discovery, using X-ray diffraction analysis, that the foulant material was an amorphous structure (no distinct size, shape or structure) (Blatchley et al., 1996; Lin et al., 1999a). Preformed particles,

such as those attributable to PO_4^{3-} precipitation, could also cause extensive fouling. Furthermore, iron was a major component of the foulant with the lamps on, but negligible with the lamps off. However aluminium was significant in both cases. The possible reasons for this are:

- For iron, it has been proved that complex organics may form when significant DOC was present in association with soluble iron in wastewater. The thermal output of the UV lamps could induce photochemical and thermal dissociation of complex organics and result in releases of iron from the complexes, which would in turn form iron-containing particles on the sleeves.

- For aluminum, it was hypothesized that preformed aluminum-containing particles resulting from the addition of aluminum salt in wastewater prior to disinfection could have been partially responsible for the accumulation of aluminum, as a result of diffusion or gravitational deposition onto quartz surfaces (Lin et al., 1999a).

It was confirmed that the physico/chemical treatment processes prior to the UV photoreactor can have a significant influence on the composition of the fouling materials (Lin et al., 1997). When metal salts, such as iron or aluminum, are added to the wastewater for coagulation and flocculation, they will become the main fouling materials (Lin et al., 1999a; Sheriff and Gehr, 2001). The former research showed that an increase in iron concentration in the wastewater resulted in an increase in concentration of every other inorganic element in the foulant, such as calcium and magnesium. Therefore, the increased iron concentrations in wastewater were definitely responsible for the initiation of the fouling observed (Pinto and Santamaria, 1999). This will be discussed in Section 2.2.3.

2.2.3 Fouling Factors

Factors such as interfacial temperature, UV intensity, hydrodynamics and flow rate, the microstructure and topography of the sleeve surface, bacteria, and wastewater quality can influence the fouling process (Correia and Snider, 1993; Lin et al., 1999b; Sheriff and Gehr, 2001).

- Temperature

Temperature is important for fouling, because it can affect the precipitation of metal complexes, which have inverse solubility (Lin et al., 1999a). A computer model (MINEQL$^+$) and laboratory experiments indicated that iron precipitation on the sleeve surface could substantially increase when temperature was increased from 10-50 °C (Sheriff and Gehr, 2001). Inorganic fouling was found to be promoted by the UV radiation. When assessing foulant materials from physico-chemical plants, Jesien (1998) observed that the foulants were composed of 80% inorganic materials. This suggested that, in agreement with Lin, 2000, inorganic foulants, the precipitation and flocculation of which was advanced by heat output of the UV lamps, contributed the majority components of foulants on the sleeve surface.

- UV intensity

A higher UV light intensity will increase inorganic fouling (Cairns, 1996; O'Brien et al., 1996), while a decreased UV intensity may promote organic fouling (Lin et al., 1999a). In general, a newly installed UV lamp will deliver a much higher UV intensity, which may initiate fouling early on. The normal life span of a UV lamp is about one year (Trojan Technologies Inc., 2002). Therefore, UV intensity is an initial factor for fouling, and the aging of UV lamps should be considered for fouling formation (Chinniah and Kwan, 1996).

- Hydrodynamics

Fouling is a complex phenomenon due to the competing factors of loading of the fouling chemicals onto the sleeve surface and removal of the chemicals by shear forces, which increase at higher flow rates (Cairns and McKee, 1996).

Both design and operation of UV disinfection systems can have an impact on fouling. Cairns (1996) claimed that when wastewater flow rate increased, a higher volume of wastewater had to be treated per UV lamp per unit of time, hence more organics and inorganics could accumulate on the sleeve surface.

Furthermore, it was found that fouling tended to increase in the longitudinal direction of flow (Cairns and McKee, 1996).

- Microstructure and topography of the sleeve surface

Even for new and clean sleeves, many small holes and pores exist irregularly on the sleeve surface. Water contained inside the porous space of the sleeve surface would be rapidly heated, thereby promoting precipitation due to the heat generated by the UV lamps. The irregular structure of the initial fouling materials would provide a larger surface area than a clean sleeve surface, thus promoting further flocculation and attachment of foulants. There is evidence that fouling was promoted under the impaction of pre-existing particles (Bott, 1995; Lin et al., 1997; Sheriff and Gehr, 2001).

During fouling, the external sleeve surface moves from a largely silica-based system to a mixed-metal, mixed-ligand system. Microscopic examination also revealed a transformation from a smooth surface to a comparatively rough surface during the fouling process. It is believed that this rough surface serves to trap more wastewater, therefore precipitation of metal-ligand combinations that are near their solubility limits is promoted in this trapped wastewater by the heat released from the UV lamps (Lin et al., 1999a).

- Bacteria

Sehnaoui (2001) claimed that a high bacterial content in wastewater appeared to accelerate the fouling process, because of the oxidizing capabilities of bacteria, as well as the presence of extracellular material, proteins, and bacteria debis. This is most likely to happen in poor quality wastewaters.

- Wastewater quality

It is known that wastewater quality will influence the fouling process. With lower wastewater quality (combined sewer overflow > primary > secondary > tertiary), and higher discharge of colloidal material from the prior processes (biofilm processes > activated sludge), there will be a higher probability that UV-absorbing organics and inorganics can adsorb onto the lamp sleeve surface and increase the fouling rate (Cairns and McKee, 1996). It was shown that the mass of foulants observed in a physico-chemical wastewater treatment plant (mainly Fe) was significantly higher than that in a biological plant (mainly Ca, Mg, and Al), due to poorer wastewater quality (Jesien, 1998).

Pinto and Santamaria (1999) investigated the influence of iron concentrations in the wastewater. It was ascertained that increased iron concentrations may cause more rapid fouling and more iron in foulants, but increased aluminum concentrations does not show this effect. Similarly, observations from a full-scale wastewater treatment plant showed that fouling occurred after ferric chloride addition, but not after aluminum addition (Black, et al., 1993; Soroushian et al., 1996).

Iron cations will undergo hydrolysis and form amorphous complexes such as ferric hydroxide and ferric phosphate (Sedlack, 1991). These could promote the fouling rate because of their inverse solubility. Thus, if iron salts were used for coagulation, iron would be the most significant cation in the fouling materials (Lin et al., 1999a). Jesien (1998) found that there was four times more iron in the foulants after ferric chloride was added.

However, there have been cases recorded where high iron concentrations did not lead to fouling. Even though ferric chloride was added into the wastewater, it did not pose any significant fouling problems (James et al., 1996; Soroushian et al., 1996). Similar results were achieved by Topnik et al. (2000), who declared that there was no increased fouling even if the iron concentration changed from 0.2 to 0.5 mg/L, and calcium was always the main fouling element. Sehnaoui (2001) also found that increased iron concentrations (from 0 to 6 mg/L) did not increase the fouling rate, and no foulants appeared at any iron concentrations. Thus, it seemed that iron alone was not the source of the fouling problem, and there was not a clear relationship between fouling and the simple measurements of iron concentrations in wastewater. Ramos (2001) claimed that the presence of iron in the wastewater does not guarantee the formation of foulants.

There are three possible explanations for this anomaly:

- The increased iron concentrations will increase fouling only in the presence of other specific chemicals. Calcium carbonate may play an important role because of forming complex compounds with iron cations under the heat of the UV lamps. The increased iron complexation may increase fouling rates, and it has been found in large concentrations in foulants (for example, by Lin et al., 1999a). Phosphorus is another factor. Different proportions of phosphorus to iron may cause various fouling rates. In one study, the greatest fouling rate was achieved when the mass proportion of phosphorus to iron was 3 to 5 (Sheriff and Gehr, 2001).

- Hydrodynamics can influence iron deposits, and in turn the fouling rates. Shear forces, which increase with higher flow rates, may prevent iron from depositing.

- pH, temperature, and natural organic matter (NOM) may change the solubility of iron cations. The influence of pH and temperature on iron cations was described by many scientists (Snoeyink and Jenkins, 1980; Benefield et al., 1982; etc.), who calculated an optimum range for decreasing the solubility of iron cations. If the operating pH and temperature of a UV system are in the appropriate range for minimum solubility of iron, the fouling rates and the iron concentrations in the foulants will increase. NOM plays an important role in the solubilization of iron cations in water (Rose et al., 1998). NOM will interact with iron cations to generate insoluble iron-NOM complexes, which affect the iron speciation in the wastewater and the functional groups in the NOM itself (Banwart, 1999; Fukushima and Tatsumi, 1999). If there are high NOM concentrations (>5mg/L) in wastewater, and UV radiation transfers iron cations in this wastewater into suitable species for reactions with NOM, insoluble iron-NOM complexes will be formed, and will deposit on the sleeve surface.

Fouling was also found to be a problem due to high hardness, which promoted scale formation (Blatchley et al., 1993). Hardness was almost always elevated in systems with high fouling rates (Sehnaoui, 2001). Thus, calcium concentrations in wastewater likely play an important role in the fouling process,

Ramos (2001) showed that when iron and calcium were added to the wastewater, calcium co-precipitated with iron complexes, which caused severe fouling. However, iron still was the major element in the foulants. On the other hand, when iron was not present in the wastewater, calcium made up the highest concentration in the foulant. In Ramos's experiments, high BOD levels (80 - 90 mg/L) were also demonstrated to be an important factor for foulant formation.

2.2.4 Cleaning Methods

- Description

Fouling necessitates the need for cleaning of the quartz sleeves to maintain optimal system efficiency and performance (Gehr and Wright, 1998). Since wastewater treatment plants vary in both scale and wastewater quality, unique methods of cleaning are devised for individual systems.

Originally, there were two ways to clean the sleeves. One was for the lamp sleeves in major installations to be cleaned by taking a UV module out of the flow channel and moving it with an overhead crane to a cleaning basin. Inside the cleaning basin, the lamps were agitated with a cleaning solution. A washdown area adjacent to the cleaning basin was used for wiping or rinsing the sleeves. The other method was in-channel cleaning, which can be achieved by draining the channel of wastewater and refilling the channel with a cleaning solution. Coarse air bubbles injected into the bottom of the channel also can be used to promote agitation. The in-channel cleaning approach is less widely used for low-pressure systems (Temmer et al., 2000). During these types of cleaning operations, the UV disinfection systems are out of service and there are high labor costs.

The design objective for modern cleaning methods is that the cleaning process occurs without disrupting the UV disinfection process, simultaneously cutting labour costs. Current cleaning methods can be divided into automated chemical/mechanical cleaning and mechanical cleaning. The complete cleaning cycle takes place with the UV disinfection systems in their normal operating position, so that the UV disinfection process is still working. For both cleaning methods, automated wipers are employed to glide over the sleeve surfaces and remove the foulants. Figure 2-1 shows an example of mechanical cleaning by wipers. Mild detergents can be used for chemical/mechanical cleaning. Phosphoric acid of pH 1-2 is also a recommended cleaning chemical (WEF, 1996; Oliver, 2002). For the foulants caused by wastewaters of poor quality, a combination of cleaning agents should be tested to find the agent most suitable for the foulant removal without producing harmful or toxic by-products (USEPA, 2002).

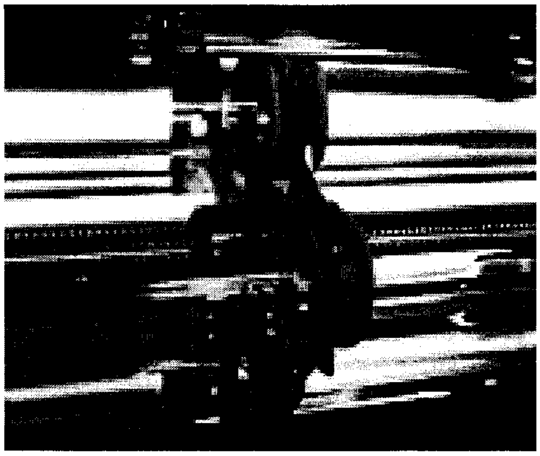

Figure 2-1 Mechanical cleaning (Source: Aquionics Inc., 2002)

Frequency of cleaning is a function of the flow capacity and the pre-treatments prior to disinfection (Gehr et al., 1993; Cairns, 1996), and is very site-specific, with some systems needing to be cleaned more often than others (USEPA, 2002).

On the other hand, it was found that fouling could be postponed somewhat by using air sparging together with proper acid immersion which could result in an increased operation time of the system before the sleeves needed cleaning (Blatchley et al., 1996). Upstream filtration may also be helpful in reducing the frequency of sleeve cleaning. Recent research has shown that the fouling process itself was also dependent on the cleaning methods used (Qiu, 2001; Oliver, 2002). Chemical/mechanical cleaning methods showed a better efficacy than mechanical methods.

- Case studies

A UV disinfection system was selected by the Gold Bar Wastewater Treatment Plant in Edmonton, Alberta, Canada. Sleeve fouling was anticipated to be a potential problem in this case, so a mechanical wiping mechanism was used for cleaning the sleeve. Sleeves were cleaned on a regular basis using an automated in-channel cleaning system where the wipers can remove the foulants. This mechanical cleaning system works well currently (USEPA, 2002).

The Ontario Centre for Environmental Technology Advancement (2002) proposes that the cleaning of the quartz sleeves can be well done by an aggressive combination of mechanical and chemical methods without interrupting normal operation. Cleaning cycles are activated by a timer or UV light sensors and are programmed to perform sequential cleaning of all modules within each operating channel. The cleaning cycle is programmed for each installation and is set as frequently as once per hour, depending on the rate of fouling. Removal of the UV systems from the channel is unnecessary except for periodic lamp replacement. When a UV lamp is to be replaced, a removal device is used to raise the height of the UV bank to a working level. A single operator can replace a lamp in minutes.

Experiments have shown that chemical/mechanical cleaning can remove the fouling materials satisfactorily (Qiu, 2001; Oliver, 2002). However, the quartz samples used in these experiments only experienced a short-term operation (less than 6 months), and wastewater quality was not taken into account. Since those experiments will have some impact on this research, they are summarized here.

Qiu (2001) found that damage to the quartz sleeves was a function of time. Over time, a decrease of UV transmittance was generated by an increase of foulants on the quartz sleeves. Moreover, the surface roughness also increased. The simple mechanical cleaning was ineffective at removing fouling materials; this was compared with the effective combinations of mechanical plus chemical cleaning. The results also showed that the dominant ions in the foulants were Fe, Al, P and Ca, with Fe being the major element. The deposited materials were amorphous solids, which were formed by precipitation at first, then sedimentation.

Oliver's (2002) article emphasized the comparison of quartz sleeve cleaning methods, which were chemical/mechanical cleaning and mechanical cleaning. The final results showed that chemical/ mechanical cleaning was effective in both wastewater field studies and drinking water field studies. With the help of scanning electron micrographs, X-ray microanalysis, and darkfield microscopy, the foulants on the quartz sleeves before and after cleaning were characterized. The results showed that chemical/mechanical cleaning can remove all the fouling materials; the quartz sleeves then had a satisfactory UV transmittance for a relatively long time without maintenance. In fact, after a two-year application and observation period, Trojan Technologies Inc. (2002) verified that the chemical/mechanical cleaning method would be effective for foulant removal. Figure 2-2 displays two different parts of one sleeve. The front section of the sleeve underwent chemical/mechanical cleaning, but the rear part did not.

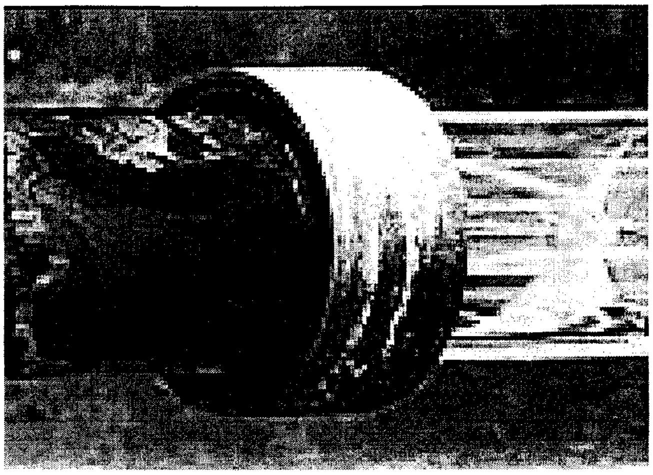

Figure 2-2 Comparison of two parts of one sleeve

(Source: Trojan Technologies Inc., 2002)

Chapter 3 Materials and Methods

3.1 Materials

The quartz sleeve samples (both used and clean samples) were collected from two sources, the Sherbrooke wastewater treatment plant (Quebec) and Trojan Technologies Inc. (London, Ontario). The used sleeve samples were from eight wastewater treatment plants with UV disinfection systems, which are represented by A, B, C, D, X, Y, Z, and S (S refers to the Sherbrooke plant). All the systems were manufactured by Trojan Technologies Inc. Key details of the UV systems are listed in Table 3-1.

Table 3-1 Key details of UV systems

UV System	**System A**	**System B**	**System C**	**System D**
Date installed	Feb-00	Apr-00	6-month pilot usage	Mar-99
Type of UV lamp	Low Pressure High Output	Low Pressure High Output	Low Pressure High Output	Low Pressure High Output
Fouling measurement method	UV Transmission (SUVT)	UV Transmission (SUVT)	UV Transmission (SUVT)	UV Transmission (SUVT)
Fouling rate	2.1 % loss of SUVT per day	3.3 % loss of SUVT per day	9.9 % loss of SUVT per day	9.4 % loss of SUVT per day
UV System	**System X**	**System Y**	**System Z**	**System S**
Date installed			Oct-00	Jul-97
Type of UV lamp	Medium Pressure	Medium Pressure	Medium Pressure	Medium Pressure
Fouling measurement method	UV Transmission (SUVT)	UV Transmission (SUVT)	UV Transmission (SUVT)	UV Transmission (SUVT)
Fouling rate	1.1 % loss of SUVT per day	9.6 % loss of SUVT per hour	2.2 % loss of SUVT per hour	

The used sleeve samples with or without any cleaning were purposely selected from eight UV disinfection systems. The properties of these sleeve samples are shown in Table 3-2. The cleaning frequency depended on the fouling rate at the site; the automated wiping systems functioned when the sleeve UV transmission (SUVT) dropped to below 95% of their original value. The chosen sleeve samples (both used and clean samples) were wrapped in lint free paper, then broken into small pieces longitudinally, and suitable ones were selected for different instrumental analyses. The pieces were cleaned by distilled water to remove non-permanent deposits. They were then air-dried. The external surfaces (convex) of the sleeve pieces were then analysed.

Table 3-2 Properties of sleeve samples

Sample	Type of UV lamp	Age	Cleaning method	Cleaning frequency	Chemical used
A*	low pressure	2.5 years	chemical/mechanical	24 hours	based on phosphoric acid
B1	low pressure	2 years	chemical/mechanical	24 hours	based on phosphoric acid
B2	low pressure	2 years	mechanical	15 minutes	
B3	low pressure	2 years	no cleaning		
C1	low pressure	6 months	chemical/mechanical	12 hours	based on phosphoric acid
C2	low pressure	6 months	mechanical	15 minutes	
C3	low pressure	6 months	no cleaning		
D1	low pressure	1 year	chemical/mechanical	12 hours	based on phosphoric acid
D2	low pressure	1 year	mechanical	15 minutes	
D3	low pressure	1 year	no cleaning		
X	medium pressure	1.5 years	chemical/mechanical	4 hours	based on phosphoric acid
Y	medium pressure	1 year	chemical/mechanical	1 hour	based on phosphoric acid
Z	medium pressure	2 years	chemical/mechanical	2 hours	based on phosphoric acid
S	medium pressure	1 year	chemical/mechanical	8 hours	phosphoric acid

* Sample A was from System A, B1~B3 were from System B, etc.

3.2 Methods

To assess the nature of the permanent foulants (permanent deposit) and the influence of different cleaning methods on the sleeves, four instrumental analyses were employed. They were Sleeve UV Transmittance (SUVT), Atomic Force Microscope (AFM), X-Ray Fluorescence (XRF), and Scanning Electron Microscope (SEM) combined with Energy Dispersive X-ray Microanalysis (EDX).

3.2.1 Sleeve UV Transmittance Test

Sleeve UV transmittance (SUVT) in this research refers to the ratio of the UV intensity through a fouled sleeve to the original UV intensity through a clean sleeve (control); it is a relative intensity, expressed as a decimal fraction. For example, if the SUVT of a control whose UV intensity is 126.8 μw/cm^2 is set as 1, then the SUVT of a fouled sleeve with a UV intensity of 125.6 μw/cm^2, is 0.99 (125.6/126.8). This test was performed in the Environmental Engineering Laboratories of the Department of Civil Engineering and Applied Mechanics at McGill University. A low pressure mercury UV lamp was used as the source of collimated UV$_{254}$ radiation. The intensity of UV radiation passing through the sleeve pieces was measured by a detector (International Light Model SEL 240) and a radiometer with a digital UV intensity display (International Light Model IL 1400A). Figure 3-1 illustrates the apparatus which was used. The distance from the lamp centre line to the sleeve sample was 375 mm. The sleeve sample was placed directly on the detector.

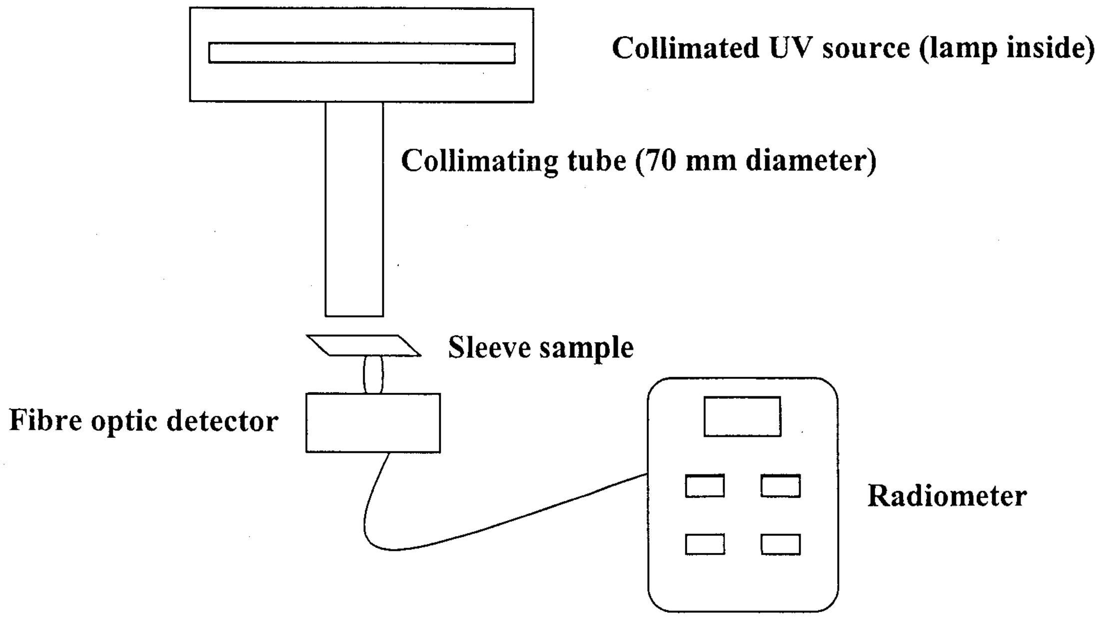

Figure 3-1 Collimated UV apparatus for testing SUVT

Since the UV intensity was not completely stable over time, it was necessary for any sample to replicate the SUVT measurements several times (at least 5 times) to arrive at a convincing average value. To decrease errors induced by system instability, preheating, zeroing and calibration were carefully done before performing SUVT measurements. Sleeve UV transmittance was measured under three types of conditions:

- Nil condition, where no sleeve samples were measured. The radiometer recorded only the UV intensity from the UV lamp directly on to the detector (through the collimating tube); it was used to determine whether the UV intensity was stable or not.

- Control condition, where the clean and unused sleeve samples (the controls) were measured. According to the two different types of sleeve samples, either from low or medium pressure UV disinfection systems, two kinds of controls were measured. The UV intensity measured in this condition was regarded as 100% UV transmittance for that kind of sleeve.

- Sample condition, where fourteen sleeve samples from different UV disinfection systems were measured. The ratio of the UV intensity of a specific sample to that of its control was considered as the SUVT of that sample.

3.2.2 Atomic Force Microscope

To determine the affect of fouling and cleaning, the roughness and morphology of the sleeve sample surfaces are the main reference terms. They were assessed by Tapping Mode Atomic Force Microscopy (AFM) (Dimension ^{TM} 3100) employed in the Department of Earth and Planetary Sciences at McGill University.

Tapping Mode AFM is also named Contact AFM. Here, a brittle tip, which is attached to the end of a cantilever with a low spring constant, makes soft physical contact with the sample surface. When the tip moves across the sample surface, the contact force will cause the cantilever to bend to accommodate changes in topography. Meanwhile, the position of the laser beam, which bounces off the back of the cantilever onto a position-sensitive photodetector, will shift and generate an electronic signal. Thus, the changes of the vertical height (roughness) and some characteristics (topography) of the sample surface will be revealed and recorded (Howland and Benatar, 1996). Roughness itself also has many variations, such as R_{max}, the maximum peak-to-valley height, R_{tm}, the mean depth of roughness, and R_q, the root-mean-square roughness. For this research, roughness means R_a, the arithmetic roughness average, which is the arithmetic average of the absolute values of the measured profile height deviations, given by:

$$R_a = \frac{1}{n}\sum_{i=1}^{n} \left| z_i - \bar{z} \right|$$

where, R_a is the arithmetic roughness average, n the number of height positions along the line profile, Z_i the height at position i and $\bar{Z}$, the average height.

Then with the help of a computer, a three-dimensional image of the sample surface will be generated. Figure 3-2 shows the movement of the tip on the sample surface.

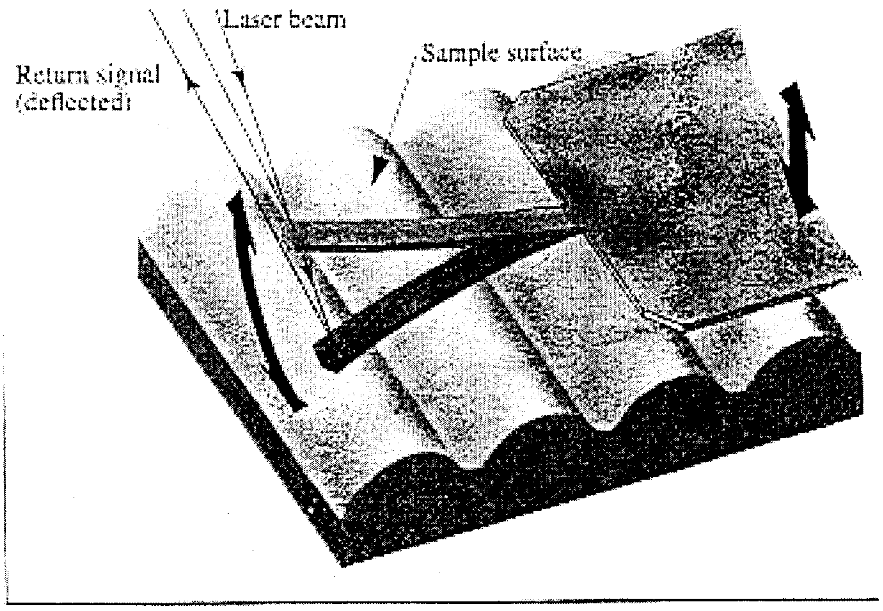

Figure 3-2 Tapping cantilever on sample surface
(Source: Digital Instruments, 1998)

The positions of the sample surface for the tip movements need to be relatively flat and clean. The reasons are as follows:

- If the sample surface is very rough, the height difference of the sample surface is excessive. When the fragile tip moves from the deepest point to the highest, it would be blocked by this highest point, then broken from the cantilever. Alternatively, when the tip moves from the highest to the lowest point, it may not touch the lower surface, hence yielding a pseudo signal.
- If the sample surface is not relatively clean, for example, if dust is present, the roughness of the sample surface will be affected, and the final results will not be real. Moreover, it would be hard to determine which spot represents the permanent deposit.
- If many foulants are attached to the tip, the tip either will be broken or will only generate morphology signals of the foulants rather than the sample surface.

- It is possible that the diameter of some valley on the sample surface is beyond the AFM scanning range, which is 30-40 μm.

3.2.3 X-ray Fluorescence

To quantitatively determine the relative weights of the components of permanent fouling, an X-ray Fluorescence spectrometer (PHILIPS PW2440 4 kW) in the Department of Earth and Planetary Sciences at McGill University was used. Figure 3-3 shows the basic structure of the XRF procedure.

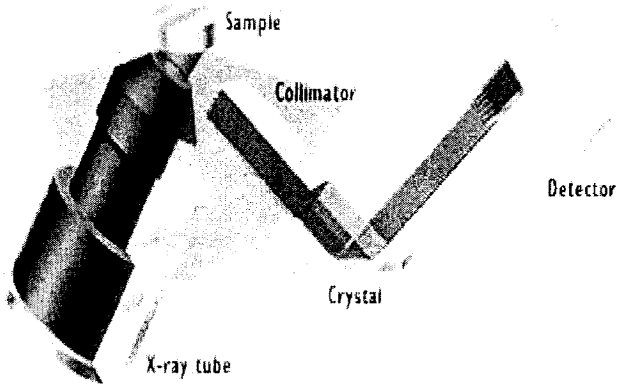

Figure 3-3 Basic structure of XRF apparatus
(Source: Royal Philips Electronics (2002), retrieved from http://www.panalytical.com/technologies/xrf**)**

An end-window x-ray tube is the source of high power x-rays for sample excitation. The primary collimator is a closely spaced parallel metal plate, which reduces beam divergence. When the sample is bombarded with x-rays, it emits secondary radiation (fluorescence) at wavelengths characteristic of each element present. The analysing crystal is a natural or synthetic material, which diffracts x-rays of differing wavelength, depending upon the angle at which the incident beam strikes. A detector converts x-ray photon energy into electrical current pulses that provide a measure of element concentration.

A sequential spectrometer enables any number and combination of elements - from Be (atomic number 4) to U (atomic number 92) and beyond - to be measured successively. It employs an optical assembly called a 'goniometer', which is equipped with two concentric, rotatable shafts. These enable the analysing crystal to turn through angular increments (theta degrees), while the detector rotates through 2-theta degrees to intercept the diffracted beam. Spectral peaks are detected at various wavelengths.

The results of continuous scanning over an angular range can be plotted as a spectral pattern, from which the elements present in a sample may be identified. Individual peak intensities are measured to determine relative masses (%) of elements. Relative mass (%) (or weight percent) is the mass of the selected element divided by the total mass of the deposit. These masses are, in turn, determined from the areas under the curves (spikes), hence the total mass is strictly only the mass of those elements which could be detected by the instrument, and not the actual mass of the foulant. Measurement times as short as 2 seconds suffice for many elements - although longer times are required for the lightest elements, which produce relatively small numbers of characteristic fluorescent photons (Department of Earth and Planetary Sciences at McGill University, 2002). XRF has its detection limits, which means XRF cannot detect the relative weight of an element below 0.01%.

3.2.4 Scanning Electron Microscope and Energy Dispersive X-ray Microanalysis

Qualitative analysis of the composition of the permanent fouling was accomplished by SEM (JEOL 840A) combined with EDX in the Department of Mining and Metallurgical Engineering at McGill University.

The combination of high resolution, an extensive magnification range, and high depth of field (the ability to maintain focus across a field of view regardless of surface roughness) makes the SEM uniquely suited for the study of surfaces (Gabriel, 1985). The SEM uses electrons for image formation, because electrons have a much shorter wavelength than light, and are capable of generating higher resolution information. Enhanced resolution in turn permits higher magnification without loss of detail. The high depth of field of SEM makes images always maintain the three-dimensional appearance of the sample surface. Figure 3-4 shows a simplified diagram of the SEM.

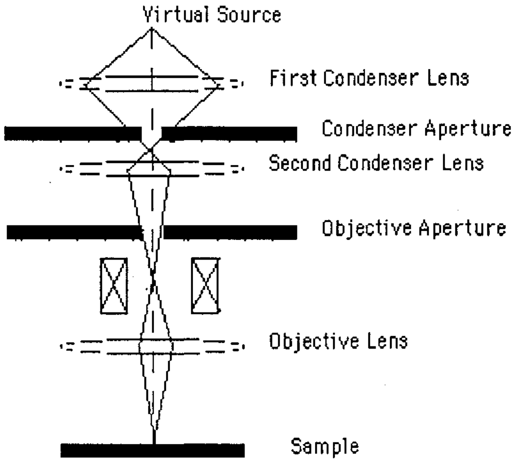

Figure 3-4 Simplified diagram of SEM
(Source: University of Nebraska at Lincoln (2002),
retrieved from http://www.unl.edu/CMRAcfem)

The "Virtual Source" at the top represents the electron gun, producing a stream of monochromatic electrons. The stream is condensed by the first condenser lens. The condenser aperture, eliminating some high-angle electrons, then constricts the beam. The second condenser lens forms the electrons into a thin, tight, coherent beam. A user-selectable objective aperture further eliminates high-angle electrons from the beam. The final lens, the Objective, focuses the scanning beam onto the part of the sample surface desired.

The SEM is equipped with a spectrometer capable of detecting X-rays emitted by the sample surface during high-energy electron beam excitation. These X-rays carry a characteristic energy and wavelength, which when measured will reveal the elemental composition of the sample surface. This technique is named Energy Dispersive X-ray

Microanalysis (Gabriel, 1985). The X-ray signal from the sample surface passes through a thin beryllium window into a cooled reverse-bias lithium-drifted silicon detector. Absorption of each individual X-ray photon leads to the ejection of a photoelectron which gives up most of its energy to the formation of electron-hole pairs. They in turn are swept away by the applied bias to form a charge pulse which is then converted to a voltage pulse by a charge-sensitive preamplifier. The signal is further amplified and shaped by a main amplifier and finally passed to a multichannel analyzer (MCA), where the pulses are sorted by voltage. The voltage distribution can be displayed on a cathode ray tube or an X-Y recorder. The contents of the MCA memory either reside directly in a computer or can be transmitted to a computer for further processing, such as peak identification of a specific element.

Before performing EDX measurements, a thin coating of a mixture of Au and Pd must be sprayed on to the sample surface to confer electrical conductivity to the sample. Figure 3-5 shows a simplified diagram of the coating machine, which was used in the Department of Mining and Metallurgical Engineering at McGill University.

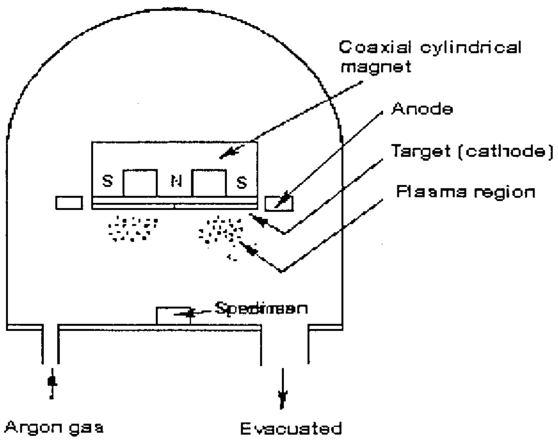

Figure 3-5 Simplified diagram of the coating machine

(Source: JEOL USA, Inc (2002), retrieved from http://www.jeol.com/sem_gde/distort.html)

Samples are placed in the chamber and the lid is closed gently. The chamber is flushed with argon 2 to 3 times using the fine gas control knob. Gas pressure in the chamber is increased with the fine gas control knob to approximately 55-70 millitorr (1 torr = 130

Pa). When the gas pressure stabilizes, the high voltage control knob is turned clockwise to achieve approximately 10 milliamperes. After that, the timer is set to the desired coating time (15 minutes). The auto-plasma will then coat samples automatically until the set time has expired.

Chapter 4 Results and Discussion

4.1 Sleeve UV Transmittance Test

The SUVT of the sleeve samples is listed in Table 4-1. Since they were measured at different times, the UV intensity for the "nil" conditions varied, which affected the values of the UV intensity transmitted by the sleeve samples. However, the difference would not influence the final SUVT value used in the figures, because SUVT is the ratio of the UV intensity of the fouled sample to that of its control.

Table 4-1 SUVT of the sleeve samples

Samples	Average UV Intensity (μw/cm^2)	SUVT	Cleaning method
Nil a	143.5		
Control Low	126.8	1	
Sample A	125.6	0.99	chemical/mechanical
Sample B1	124.5	0.98	chemical/mechanical
Sample B2	38.7	0.31	mechanical
Sample B3	20.2	0.16	no cleaning
Sample C1	123.4	0.97	chemical/mechanical
Sample C2	36.1	0.28	mechanical
Sample C3	27.5	0.22	no cleaning
Sample D1	122.8	0.97	chemical/mechanical
Sample D2	40.4	0.32	mechanical
Sample D3	13.9	0.11	no cleaning
Nil b	144.5		
Control Medium	127.3	1	
Sample X1	126.4	0.99	chemical/mechanical
Sample X2	40.6	0.32	chemical/mechanical
Sample Y	124.4	0.977	chemical/mechanical
Sample Z	125.2	0.984	chemical/mechanical
Nil c	147.2		
Control S	126.5	1	
Sample S	118.4	0.94	chemical/mechanical

From Table 4-1, it is shown that sleeve samples undergoing chemical/mechanical cleaning have relatively higher SUVT values than those experiencing only mechanical cleaning. After similar chemical/mechanical cleaning (based on phosphoric acid), Samples X1, Y and Z display higher SUVT than Sample S, although they all came from medium pressure UV disinfection systems.

- Figure 4-1 shows comparisons of SUVT among the sleeve samples from low pressure UV systems.

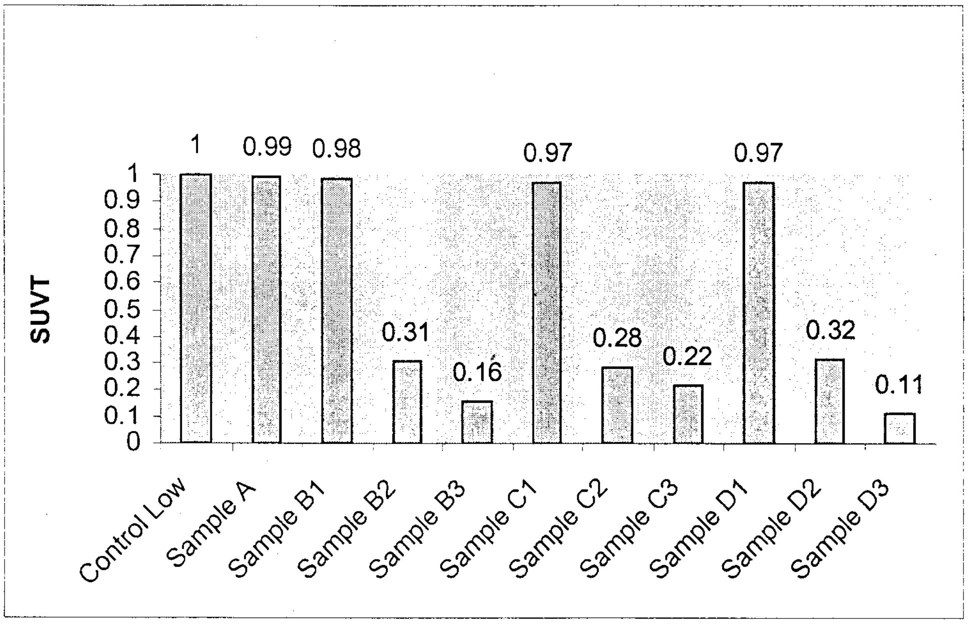

Figure 4-1 SUVT of the sleeve samples from low pressure UV systems

Samples A, B1, C1, and D1, after chemical/mechanical cleaning, have satisfactory SUVT (> 95%). However the SUVT of Samples B2, C2, and D2 after mechanical cleaning, drops sharply. Thus, it can be concluded that chemical/mechanical cleaning is more effective in foulant removal. Samples B3, C3, and D3 without any cleaning were wrapped by foulants, and their SUVT was almost negligible.

There appears to be no clear relationship between the ages of the sleeve samples (with or without cleaning) and their SUVT. For example, although Samples A and B1 were used for more than two years, after similar chemical/mechanical cleaning, their SUVT is evidently higher than that of Sample C1 (only 6 months) and Sample D1 (1 year). Also, Sample B2 (2 years) after mechanical cleaning has a similar SUVT as Sample C2 (6 months).

On the other hand, the site specific fouling rates can affect their SUVT: Sample A (2.1 % loss of SUVT/day) and Sample B1 (3.3 % loss of SUVT/day) with lower fouling rates have higher SUVT, compared to Sample C1 (9.9 % loss of SUVT/day) or Sample D1 (9.4 % loss of SUVT/day) with higher fouling rates and lower SUVT.

Concurrently, the intervals of chemical/mechanical cleaning of Samples A and B1 (24 hours) with higher SUVT are longer than those of Samples C1 and D1 (12 hours) which have lower SUVT. However, the intervals of mechanical cleaning of Samples B2, C2, and D2 are the same (15 minutes), and the SUVT of these samples is very similar.

- Figure 4-2 shows the SUVT of the sleeve samples from medium pressure UV systems

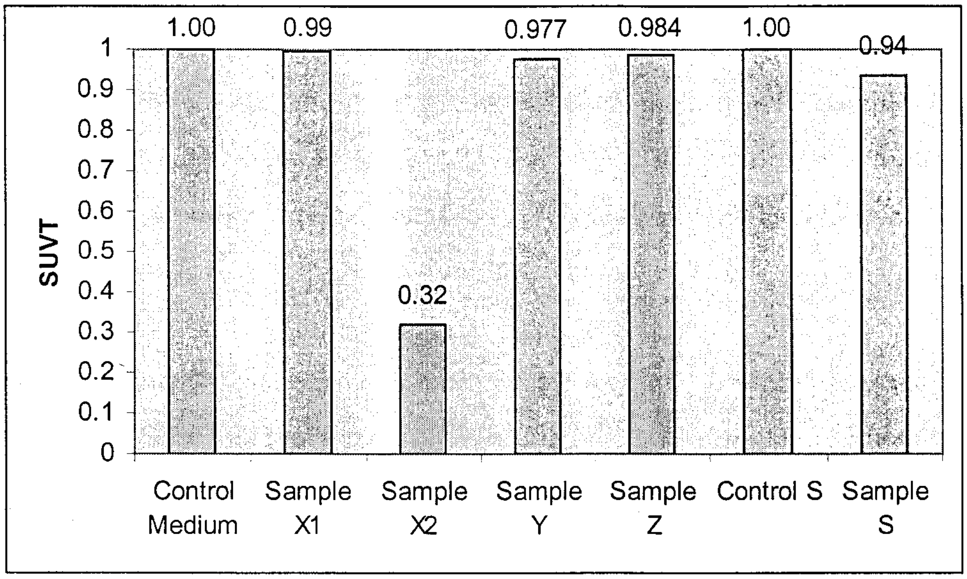

Figure 4-2 SUVT of the sleeve samples from medium pressure UV systems

All samples were cleaned by their site specific chemical/mechanical cleaning systems. Samples X1, Y, and Z display satisfactory SUVT, which is more than 95%. However, Sample X2 shows a very poor SUVT, although it came from the same sleeve as Sample X1. The difference may be attributed to an unsuitable cleaning system, which only performed well on parts of the sleeve. Moreover, because the SUVT of X2 is very similar to that of Samples B2, C2, and D2, which experienced mechanical cleaning, it can be deduced reasonably that Sample X2 was not reached by the cleaning chemicals and was only mechanically cleaned. Thus, to determine the effects of chemical/mechanical cleaning, only Samples X1, Y, and Z are focused on.

Similarly, the SUVT of the sleeve samples cannot be correlated to their ages, since Sample Y (1 year) has a lower SUVT than Sample Z (2 years). Samples Y and Z have much higher fouling rates (9.6 % loss of SUVT/hour and 2.2 % loss of SUVT/hour, respectively) than Sample X1 (1.1 % loss of SUVT/day), which lead to the lower SUVT of Samples Y and Z, and more frequent cleaning.

After chemical/mechanical cleaning, the SUVT of Sample S was moderate, which is lower than other samples from similar medium pressure UV systems to System S. Although the fouling rate was not measured, the frequency of the cleaning of Sample S was lower than that of other sleeve samples from medium pressure UV systems, which may be the reason for the lower SUVT. However, System S always had a good disinfecting efficacy, even though the SUVT of the sleeve is only moderate.

In general, the SUVT tests verified that chemical/mechanical cleaning is more effective than mechanical cleaning itself. It is not the ages of the sleeves but the fouling rates that influence the SUVT of the sleeves. The fouling rates can affect SUVT, and in turn the intervals of chemical/mechanical cleaning. The fouling rates are site specific, which may be ascribed to differences in wastewater quality at the different sites. On the other hand, although chemical/mechanical cleaning is useful, the SUVT of the sleeve samples after a long period of application cannot regain 100% SUVT, which means that there are always foulants remaining (permanent fouling) which reduce the SUVT of the sleeves.

4.2 Topography and Roughness

The topography and roughness of the sleeve samples were measured by the Atomic Force Microscope (AFM). It was time-consuming work, because there were many known and unknown factors adversely influencing the sensitive AFM, which caused unreal or false signals ("noise"). Moreover, AFM can only measure a very small area of a specific sample. Thus, to make the final results reasonable, a single sample was measured repeatedly (at least 3 times) at different relatively flat and clean areas.

- Sleeve samples from low pressure UV systems

The topography and roughness of the sleeve samples from low pressure UV systems are shown in Figures 4-3, a ~ k.

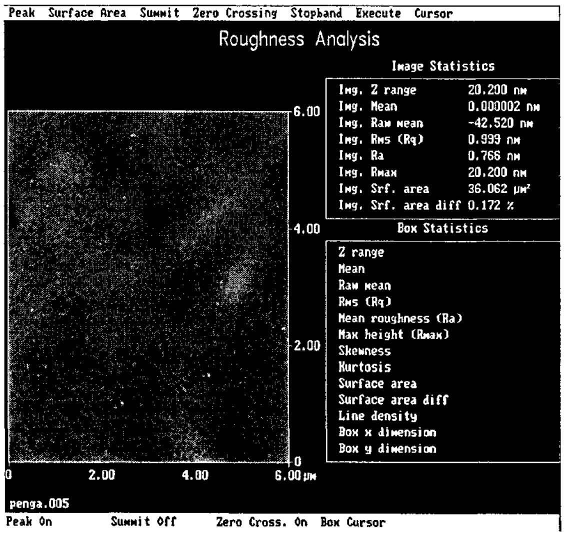

```
Image Statistics
Img. Z range           20.200 nm
Img. Mean              0.000002 nm
Img. Raw mean          -42.520 nm
Img. Rms (Rq)          0.999 nm
Img. Ra                0.766 nm
Img. Rmax              20.200 nm
Img. Srf. area         36.062 μm²
Img. Srf. area diff    0.172 %
Box Statistics
Z range
Mean
Raw mean
Rms (Rq)
Mean roughness (Ra)
Max height (Rmax)
Skewness
Kurtosis
Surface area
Surface area diff
Line density
Box x dimension
Box y dimension
```

a. Control Low

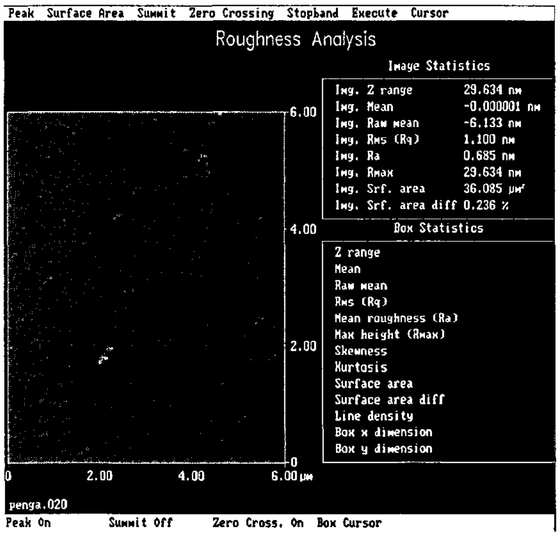

```
Image Statistics
Img. Z range           29.634 nm
Img. Mean              -0.000001 nm
Img. Raw mean          -6.133 nm
Img. Rms (Rq)          1.100 nm
Img. Ra                0.685 nm
Img. Rmax              29.634 nm
Img. Srf. area         36.085 μm²
Img. Srf. area diff    0.236 %
Box Statistics
Z range
Mean
Raw mean
Rms (Rq)
Mean roughness (Ra)
Max height (Rmax)
Skewness
Kurtosis
Surface area
Surface area diff
Line density
Box x dimension
Box y dimension
```

b. Sample A

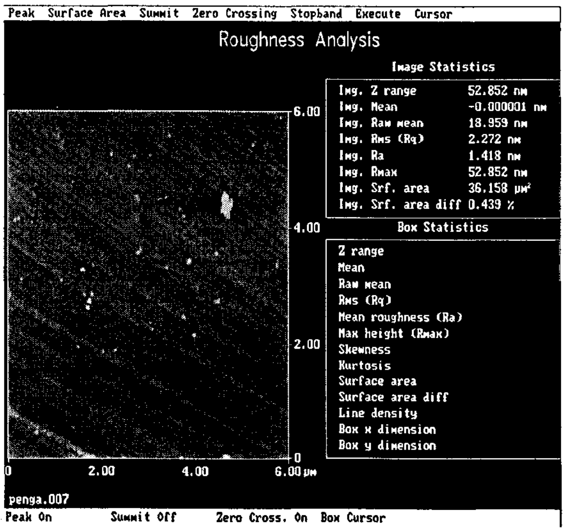

```
Image Statistics
Img. Z range           52.852 nm
Img. Mean              -0.000001 nm
Img. Raw mean          18.959 nm
Img. Rms (Rq)          2.272 nm
Img. Ra                1.418 nm
Img. Rmax              52.852 nm
Img. Srf. area         36.158 μm²
Img. Srf. area diff    0.439 %
Box Statistics
Z range
Mean
Raw mean
Rms (Rq)
Mean roughness (Ra)
Max height (Rmax)
Skewness
Kurtosis
Surface area
Surface area diff
Line density
Box x dimension
Box y dimension
```

c. Sample B1

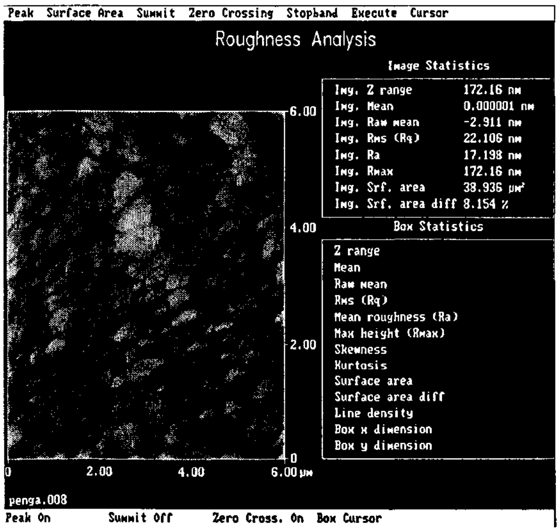

```
Image Statistics
Img. Z range           172.16 nm
Img. Mean              0.000001 nm
Img. Raw mean          -2.911 nm
Img. Rms (Rq)          22.106 nm
Img. Ra                17.198 nm
Img. Rmax              172.16 nm
Img. Srf. area         38.936 μm²
Img. Srf. area diff    8.154 %
Box Statistics
Z range
Mean
Raw mean
Rms (Rq)
Mean roughness (Ra)
Max height (Rmax)
Skewness
Kurtosis
Surface area
Surface area diff
Line density
Box x dimension
Box y dimension
```

d. Sample B2

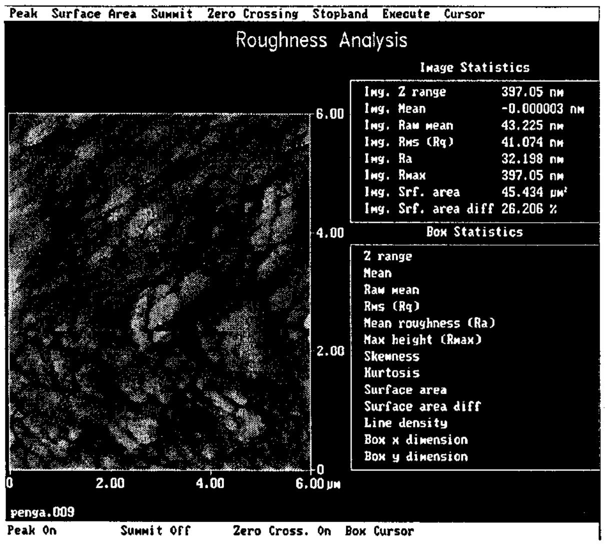

Image Statistics

Img. Z range	397.05 nm
Img. Mean	-0.000003 nm
Img. Raw mean	43.225 nm
Img. Rms (Rq)	41.074 nm
Img. Ra	32.198 nm
Img. Rmax	397.05 nm
Img. Srf. area	45.434 µm²
Img. Srf. area diff	26.206 %

Box Statistics

Z range
Mean
Raw mean
Rms (Rq)
Mean roughness (Ra)
Max height (Rmax)
Skewness
Kurtosis
Surface area
Surface area diff
Line density
Box x dimension
Box y dimension

e. Sample B3

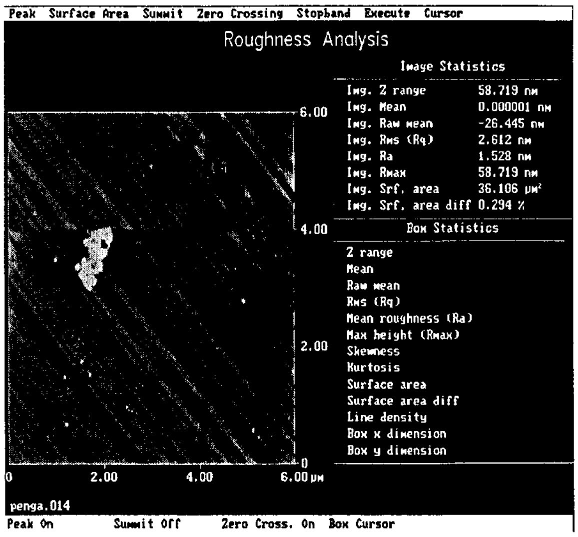

Image Statistics

Img. Z range	58.719 nm
Img. Mean	0.000001 nm
Img. Raw mean	-26.445 nm
Img. Rms (Rq)	2.612 nm
Img. Ra	1.528 nm
Img. Rmax	58.719 nm
Img. Srf. area	36.106 µm²
Img. Srf. area diff	0.294 %

Box Statistics

Z range
Mean
Raw mean
Rms (Rq)
Mean roughness (Ra)
Max height (Rmax)
Skewness
Kurtosis
Surface area
Surface area diff
Line density
Box x dimension
Box y dimension

f. Sample C1

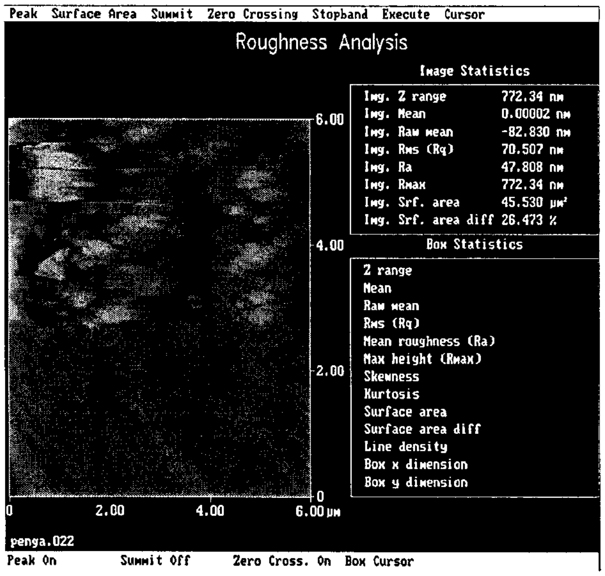

Image Statistics

Img. Z range	772.34 nm
Img. Mean	0.00002 nm
Img. Raw mean	-82.830 nm
Img. Rms (Rq)	70.507 nm
Img. Ra	47.808 nm
Img. Rmax	772.34 nm
Img. Srf. area	45.530 µm²
Img. Srf. area diff	26.473 %

Box Statistics

Z range
Mean
Raw mean
Rms (Rq)
Mean roughness (Ra)
Max height (Rmax)
Skewness
Kurtosis
Surface area
Surface area diff
Line density
Box x dimension
Box y dimension

g. Sample C2

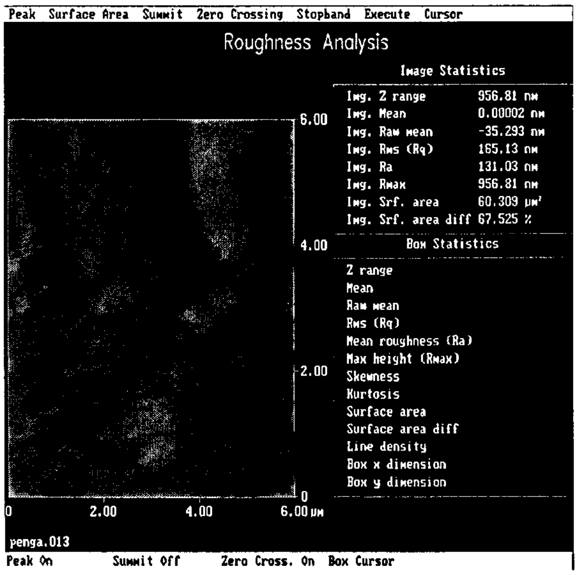

Image Statistics

Img. Z range	956.81 nm
Img. Mean	0.00002 nm
Img. Raw mean	-35.293 nm
Img. Rms (Rq)	165.13 nm
Img. Ra	131.03 nm
Img. Rmax	956.81 nm
Img. Srf. area	60.309 µm²
Img. Srf. area diff	67.525 %

Box Statistics

Z range
Mean
Raw mean
Rms (Rq)
Mean roughness (Ra)
Max height (Rmax)
Skewness
Kurtosis
Surface area
Surface area diff
Line density
Box x dimension
Box y dimension

h. Sample C3

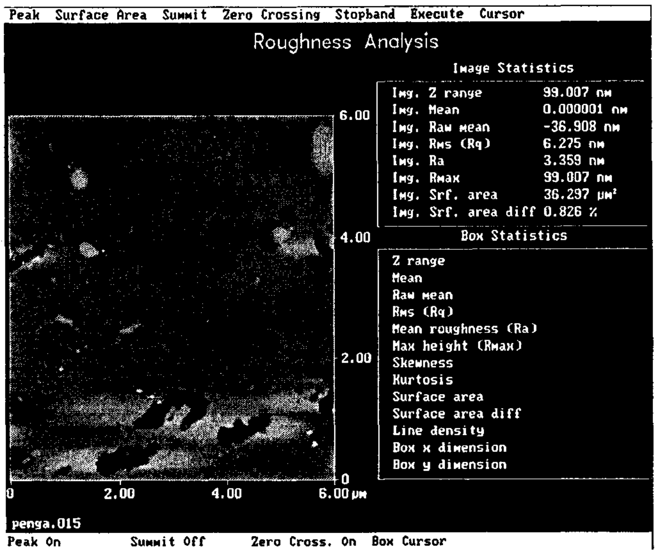

```
Image Statistics
Img. Z range          99.007 nm
Img. Mean             0.000001 nm
Img. Raw mean         -36.908 nm
Img. Rms (Rq)         6.275 nm
Img. Ra               3.359 nm
Img. Rmax             99.007 nm
Img. Srf. area        36.297 μm²
Img. Srf. area diff   0.826 %
Box Statistics
Z range
Mean
Raw mean
Rms (Rq)
Mean roughness (Ra)
Max height (Rmax)
Skewness
Kurtosis
Surface area
Surface area diff
Line density
Box x dimension
Box y dimension
```

i. Sample D1

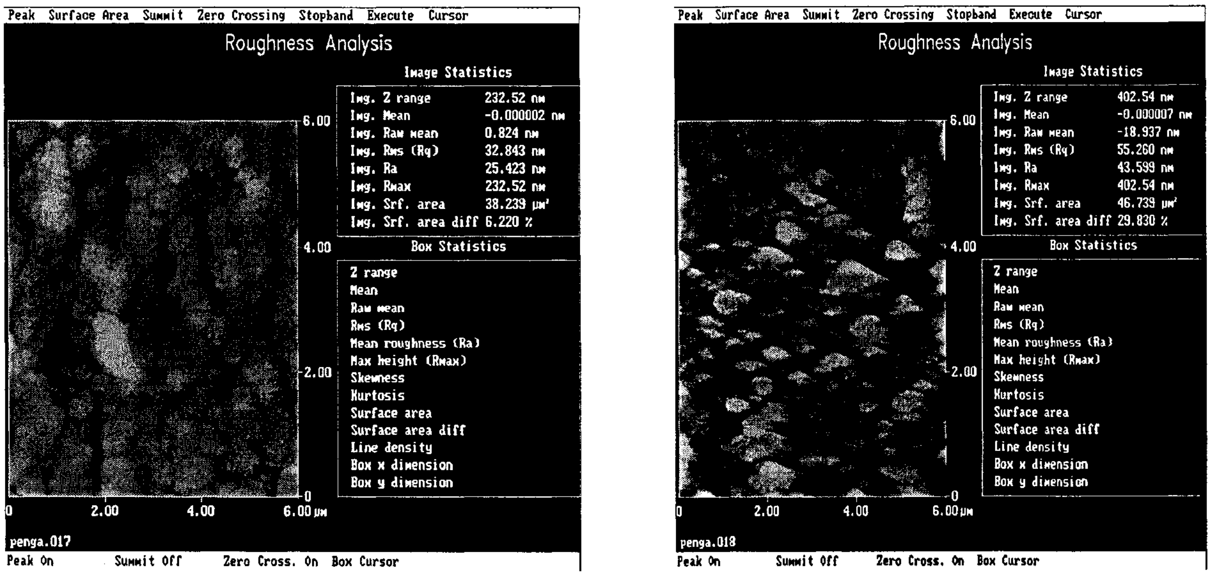

```
Image Statistics
Img. Z range          232.52 nm
Img. Mean             -0.000002 nm
Img. Raw mean         0.824 nm
Img. Rms (Rq)         32.843 nm
Img. Ra               25.423 nm
Img. Rmax             232.52 nm
Img. Srf. area        38.239 μm²
Img. Srf. area diff   6.220 %
Box Statistics
Z range
Mean
Raw mean
Rms (Rq)
Mean roughness (Ra)
Max height (Rmax)
Skewness
Kurtosis
Surface area
Surface area diff
Line density
Box x dimension
Box y dimension
```

```
Image Statistics
Img. Z range          402.54 nm
Img. Mean             -0.000007 nm
Img. Raw mean         -18.937 nm
Img. Rms (Rq)         55.260 nm
Img. Ra               43.599 nm
Img. Rmax             402.54 nm
Img. Srf. area        46.739 μm²
Img. Srf. area diff   29.830 %
Box Statistics
Z range
Mean
Raw mean
Rms (Rq)
Mean roughness (Ra)
Max height (Rmax)
Skewness
Kurtosis
Surface area
Surface area diff
Line density
Box x dimension
Box y dimension
```

j. Sample D2

k. Sample D3

Figure 4-3 Topography and roughness of the sleeve samples from low pressure UV systems

Figure 4-3 a. shows the surface of the control. From the picture, although the control is clean and unused, there are many holes and peaks on the surface, which are represented by darkness and brightness respectively. These holes and peaks will be the positions for the accumulation of foulant.

Figures 4-3 b., c., f., and i. are the surfaces of the sleeve samples after chemical/mechanical cleaning. After cleaning, the surface of Sample A is relatively plain, and the roughness is similar to that of the control. However, the minute foulants are still visible and distributed over the entire sample surface. These foulants cannot be removed completely because they are trapped in the holes or attached tightly to the peaks and the sleeve surfaces, so that they are called "permanent foulants (herein referred to as Type I)". In contrast, the surfaces of Samples B1, C1, and D1 are radically changed. The apparent parallel scratches are displayed on the surfaces of Samples B1 and C1. These scratches may be attributed to the mechanical cleaning where the wipers slid over the sleeve surfaces to remove the foulants but damaged the sleeve surface concurrently. Thus, the foulants are trapped more readily by these scratches which have wider areas, and they cannot be removed completely. Moreover, the surface of Sample D1 is damaged more severely, because there are many obvious deep holes caused by the mechanical cleaning. These holes are distributed randomly over the sleeve surface. The permanent foulants are either trapped by these holes or concentrated around these holes. Thus, the roughness of Sample D1 is the highest among these samples undergoing chemical/mechanical cleaning.

Figures 4-3 d., g., and j. show the topography of the sleeve samples after mechanical cleaning. Although Samples B2, C2 and D2 were frequently cleaned (every 15 minutes), the foulants were still attached to and covered the entire surface of the samples. These foulants can also be regarded as "permanent foulants (herein referred to as Type II)". Therefore, it can be concluded that mechanical cleaning itself is not effective for removing the foulants, even over a short term of application (Sample C2 was only employed for six months, but has a very high roughness).

Figures 4-3 e., h., and k. are the surfaces of the sleeve samples without any cleaning after use. The sleeve surfaces of Samples B3, C3, and D3 cannot be analysed, because the foulants covered the surfaces densely, and blocked most of the UV radiation.

Since chemical/mechanical cleaning is more effective than mechanical cleaning, only chemical/mechanical cleaning will be emphasized in this research. Hence, Type I permanent fouling on the sleeve surfaces (foulants induced by chemical/mechanical cleaning) will be investigated in the following sections.

Table 4-2 lists the roughness of Samples A, B1, C1, and D1.

Table 4-2 Roughness of Samples A, B1, C1, and D1

Sample	Roughness (nm)
Sample A	29.6
Sample B1	52.9
Sample C1	58.7
Sample D1	99.0

The roughness of each sample is very compatible with its topography. When the sleeve surface is not mechanically damaged, there is little permanent fouling, (being due to inherent holes and peaks on the sleeve surface), and the roughness is low. On the other hand, if the mechanical cleaning caused damage to the sleeve surface, such as scratches and holes, permanent fouling would increase dramatically and in turn raise the roughness.

This result is also compatible with the measurements of SUVT of these sleeve samples. Sample A has a lower roughness, so that it has a higher SUVT. In contrast, Sample D1 has the highest roughness, and as a result, its SUVT is the lowest among these four samples.

- Sleeve samples from medium pressure UV systems

The topography and roughness of the sleeve samples from medium pressure UV systems are shown in Figures 4-4, a ~ g.

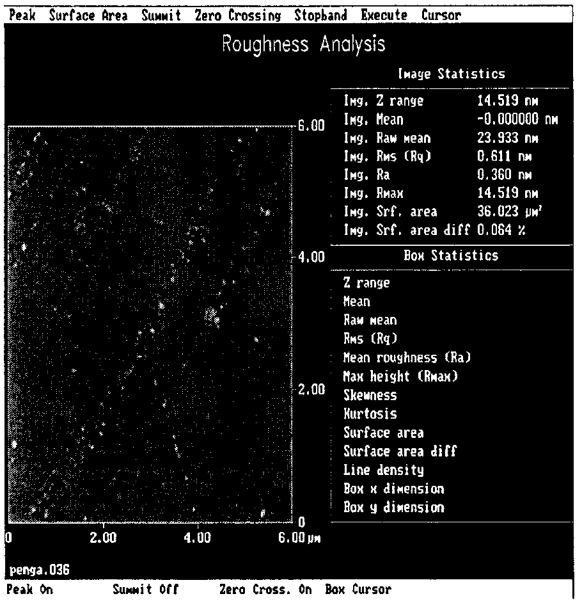

```
Image Statistics
Img. Z range           14.519 nm
Img. Mean              -0.000000 nm
Img. Raw mean          23.933 nm
Img. Rms (Rq)          0.611 nm
Img. Ra                0.360 nm
Img. Rmax              14.519 nm
Img. Srf. area         36.023 µm²
Img. Srf. area diff 0.064 %
Box Statistics
Z range
Mean
Raw mean
Rms (Rq)
Mean roughness (Ra)
Max height (Rmax)
Skewness
Kurtosis
Surface area
Surface area diff
Line density
Box x dimension
Box y dimension
```

a. Control Medium

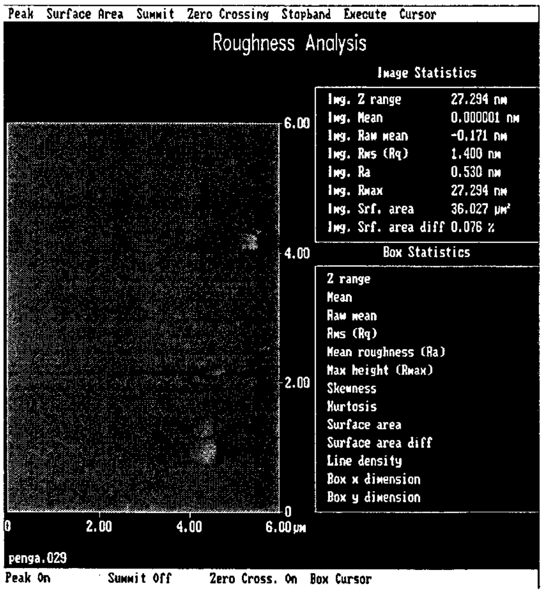

```
Image Statistics
Img. Z range           27.294 nm
Img. Mean              0.000001 nm
Img. Raw mean          -0.171 nm
Img. Rms (Rq)          1.400 nm
Img. Ra                0.530 nm
Img. Rmax              27.294 nm
Img. Srf. area         36.027 µm²
Img. Srf. area diff 0.076 %
Box Statistics
Z range
Mean
Raw mean
Rms (Rq)
Mean roughness (Ra)
Max height (Rmax)
Skewness
Kurtosis
Surface area
Surface area diff
Line density
Box x dimension
Box y dimension
```

b. Sample X1

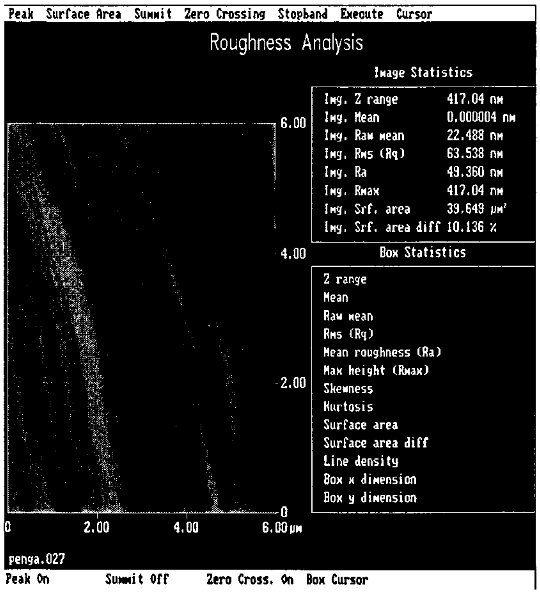

```
Image Statistics
Img. Z range           417.04 nm
Img. Mean              0.000004 nm
Img. Raw mean          22.488 nm
Img. Rms (Rq)          63.538 nm
Img. Ra                49.360 nm
Img. Rmax              417.04 nm
Img. Srf. area         39.649 µm²
Img. Srf. area diff 10.136 %
Box Statistics
Z range
Mean
Raw mean
Rms (Rq)
Mean roughness (Ra)
Max height (Rmax)
Skewness
Kurtosis
Surface area
Surface area diff
Line density
Box x dimension
Box y dimension
```

c. Sample X2

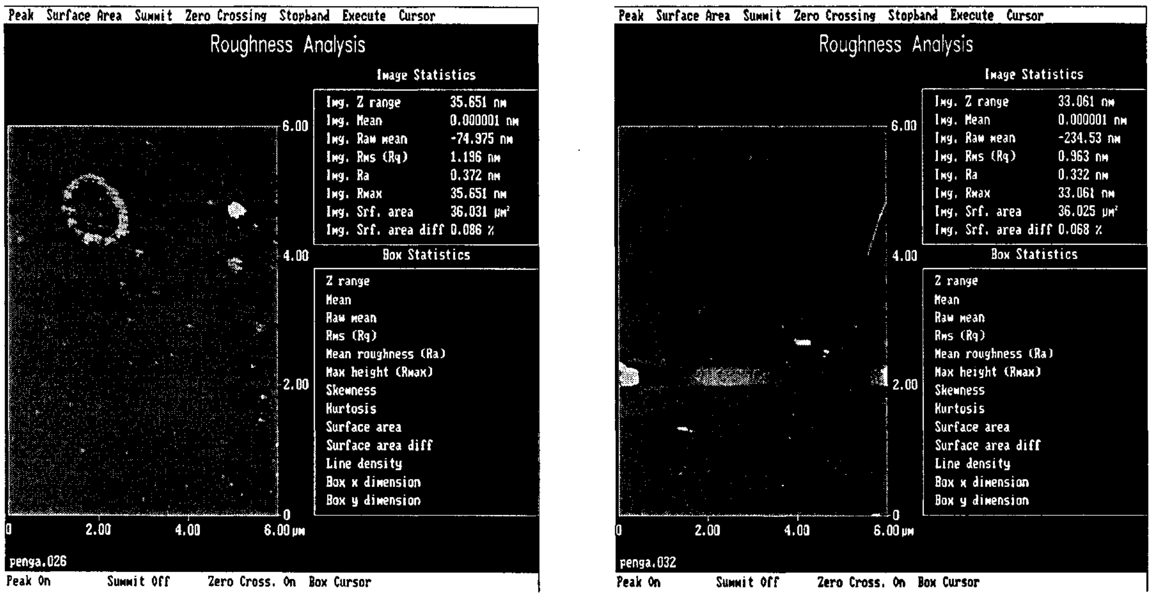

```
Image Statistics
Img. Z range            35.651 nm
Img. Mean               0.000001 nm
Img. Raw mean           -74.975 nm
Img. Rms (Rq)           1.196 nm
Img. Ra                 0.372 nm
Img. Rmax               35.651 nm
Img. Srf. area          36.031 µm²
Img. Srf. area diff 0.086 %
Box Statistics
Z range
Mean
Raw mean
Rms (Rq)
Mean roughness (Ra)
Max height (Rmax)
Skewness
Kurtosis
Surface area
Surface area diff
Line density
Box x dimension
Box y dimension
```

```
Image Statistics
Img. Z range            33.061 nm
Img. Mean               0.000001 nm
Img. Raw mean           -234.53 nm
Img. Rms (Rq)           0.963 nm
Img. Ra                 0.332 nm
Img. Rmax               33.061 nm
Img. Srf. area          36.025 µm²
Img. Srf. area diff 0.068 %
Box Statistics
Z range
Mean
Raw mean
Rms (Rq)
Mean roughness (Ra)
Max height (Rmax)
Skewness
Kurtosis
Surface area
Surface area diff
Line density
Box x dimension
Box y dimension
```

d. Sample Y

e. Sample Z

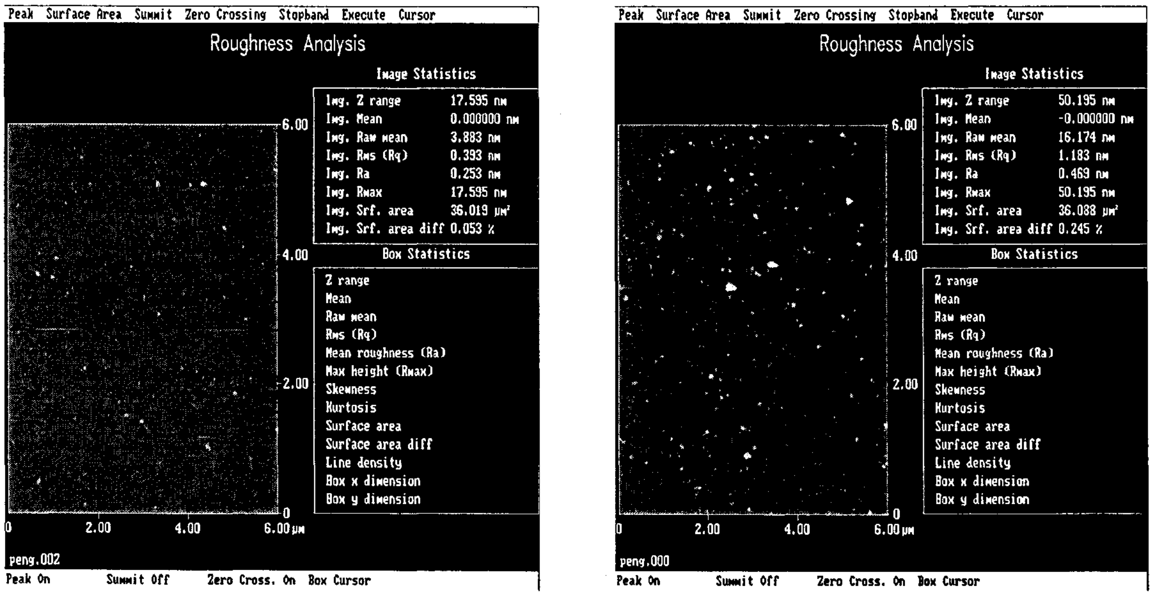

```
Image Statistics
Img. Z range            17.595 nm
Img. Mean               0.000000 nm
Img. Raw mean           3.883 nm
Img. Rms (Rq)           0.393 nm
Img. Ra                 0.253 nm
Img. Rmax               17.595 nm
Img. Srf. area          36.019 µm²
Img. Srf. area diff 0.053 %
Box Statistics
Z range
Mean
Raw mean
Rms (Rq)
Mean roughness (Ra)
Max height (Rmax)
Skewness
Kurtosis
Surface area
Surface area diff
Line density
Box x dimension
Box y dimension
```

```
Image Statistics
Img. Z range            50.195 nm
Img. Mean               -0.000000 nm
Img. Raw mean           16.174 nm
Img. Rms (Rq)           1.183 nm
Img. Ra                 0.469 nm
Img. Rmax               50.195 nm
Img. Srf. area          36.088 µm²
Img. Srf. area diff 0.245 %
Box Statistics
Z range
Mean
Raw mean
Rms (Rq)
Mean roughness (Ra)
Max height (Rmax)
Skewness
Kurtosis
Surface area
Surface area diff
Line density
Box x dimension
Box y dimension
```

f. Control S

g. Sample S

Figure 4-4 Topography and roughness of the sleeve samples from medium pressure UV systems

Figure 4-4 a. is the surface of the control. It is obvious that there are many small inherent holes and peaks spread over the control surface. Figures 4-4 b., c., d., and e. show the surfaces of the sleeve samples after chemical/mechanical cleaning. Samples X1 and X2 came from the same sleeve, but the roughness is very different. The surface of Sample X1 was not damaged seriously, thus only a few permanent foulants deposited on it. On the other hand, the surface of Sample X2 was severely impaired, which could be ascribed to the mechanical cleaning and the absence of cleaning chemicals, so that dense foulants were attached to the sleeve surface and increased the roughness.

There are apparent scratches on the surfaces of Samples Y and Z. These scratches were likely also caused by the mechanical cleaning. Although chemical/mechanical cleaning can remove most of the foulants, there are still permanent foulants trapped by the scratches that have wide surface areas. It is apparent from Figures 4-4 d. and e. that the foulants scatter in accordance with these scratches.

Figure 4-4 f. is the surface of Control S. It can be seen that many holes and peaks, to which the foulants can be attached, cover the surface of the control. Figure 4-4 g. shows the surface of Sample S where the scratches are very evident and distributed vertically and horizontally. Therefore, more foulants are trapped or attached to these scratches, which will in turn augment the roughness. The high roughness results in only moderate SUVT.

Table 4-3 lists the roughness of Samples X1, X2, Y, Z and S. The roughness of Samples X1 and X2 is in agreement with the results of SUVT. Sample X1 has a lower roughness but higher SUVT, while Sample X2 has a lower SUVT because of the higher roughness. Moreover, Samples Y and Z have higher roughness than Sample X1, which lead to the lower SUVT of Samples Y and Z.

Table 4-3 Roughness of Samples X1, X2, Y, Z and S

Sample	Roughness (nm)
Sample X1	27.3
Sample X2	417
Sample Y	35.6
Sample Z	33.1
Sample S	50.2

Basically, chemical/mechanical cleaning is effective in removing the foulants. However, because of the inherent holes and peaks on the sleeve surface, there will always be foulants which remain trapped by these holes which have wide surface areas. Mechanical cleaning can damage the sleeve surface severely, causing scratches or even holes (called "mechanical deterioration of the sleeves"). Thus mechanical cleaning can increase the permanent fouling, and this fouling cannot be avoided. It was also shown that the site specific chemical/mechanical cleaning methods can induce different levels of permanent fouling.

Mechanical damage of the surfaces of the sleeves undergoing chemical/mechanical cleaning appears to be less than that on the sleeves experiencing only mechanical cleaning. This could be due to the longer intervals for chemical/mechanical cleaning than those for mechanical cleaning, and/or that if mechanical cleaning is used alone, it needs to be harsher than if it is combined with chemical cleaning.

4.3 Qualitative Analyses

The qualitative analyses show the compositions of the foulants, and the proportion of a specific chemical in the foulants. To determine the components of the foulants, a Scanning Electron Microscope (SEM) associated with Energy Dispersive X-ray Microanalysis (EDX) was used.

- Sleeve samples from low pressure UV systems

The compositions of the foulants on the sleeves from low pressure UV systems are shown in Figures 4-5, a ~ k.

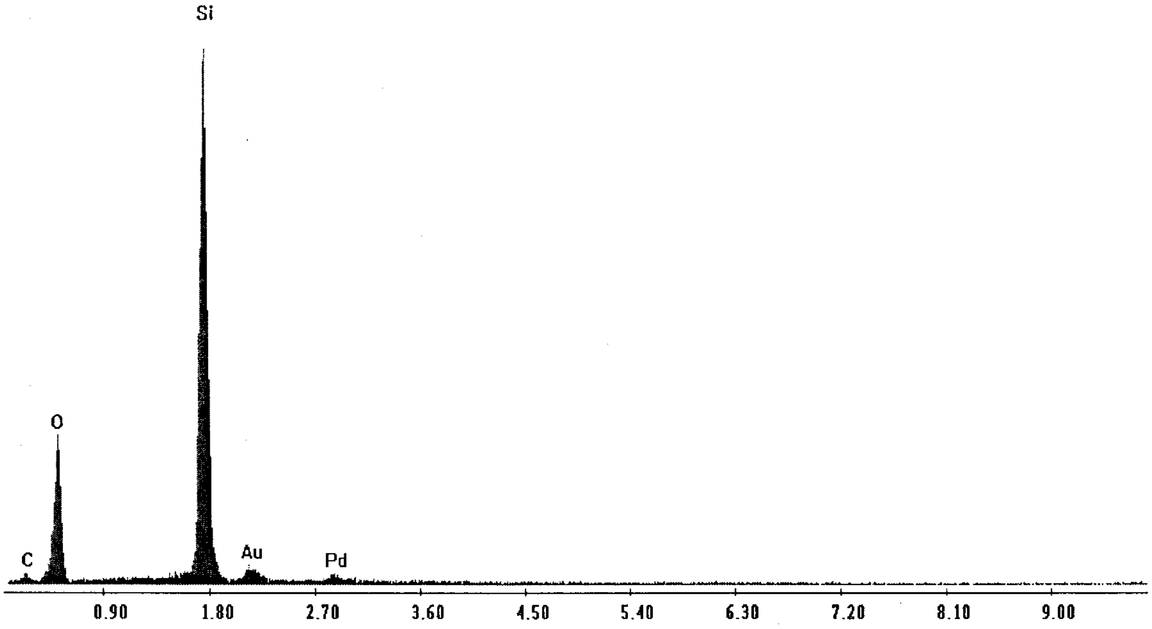

a. Control Low

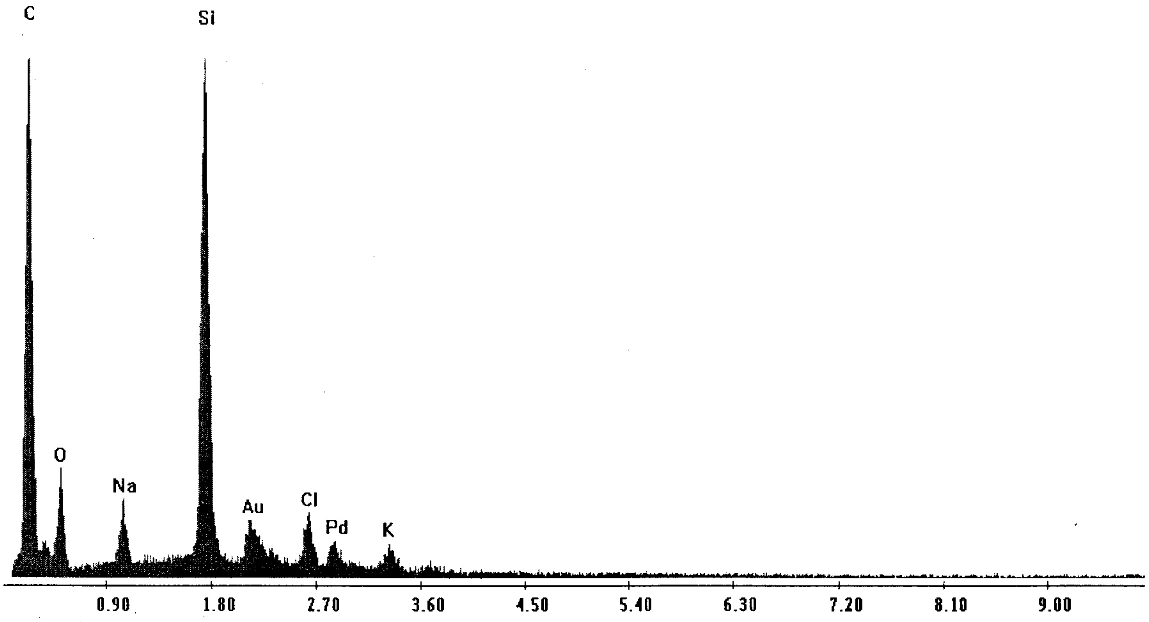

b. Sample A

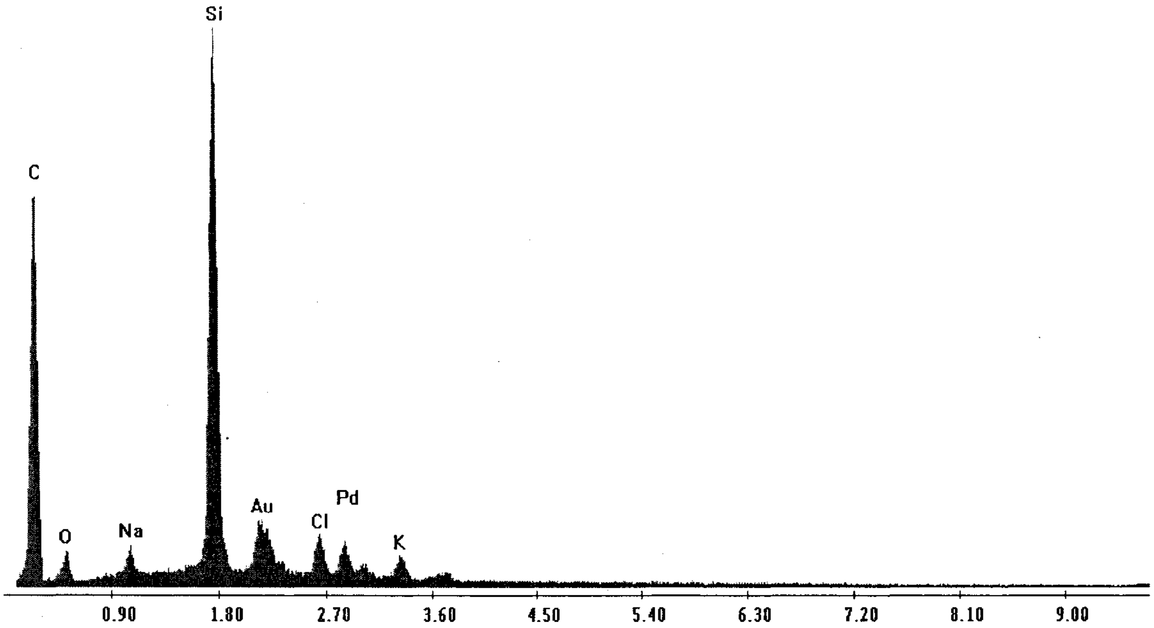

c. Sample B1

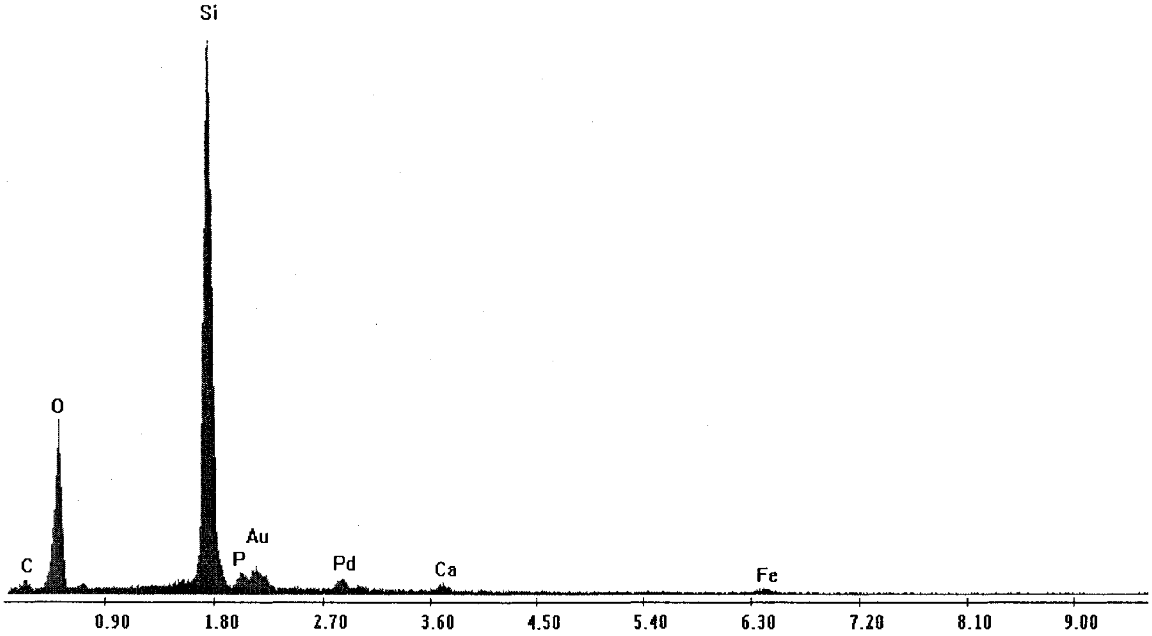

d. Sample B2

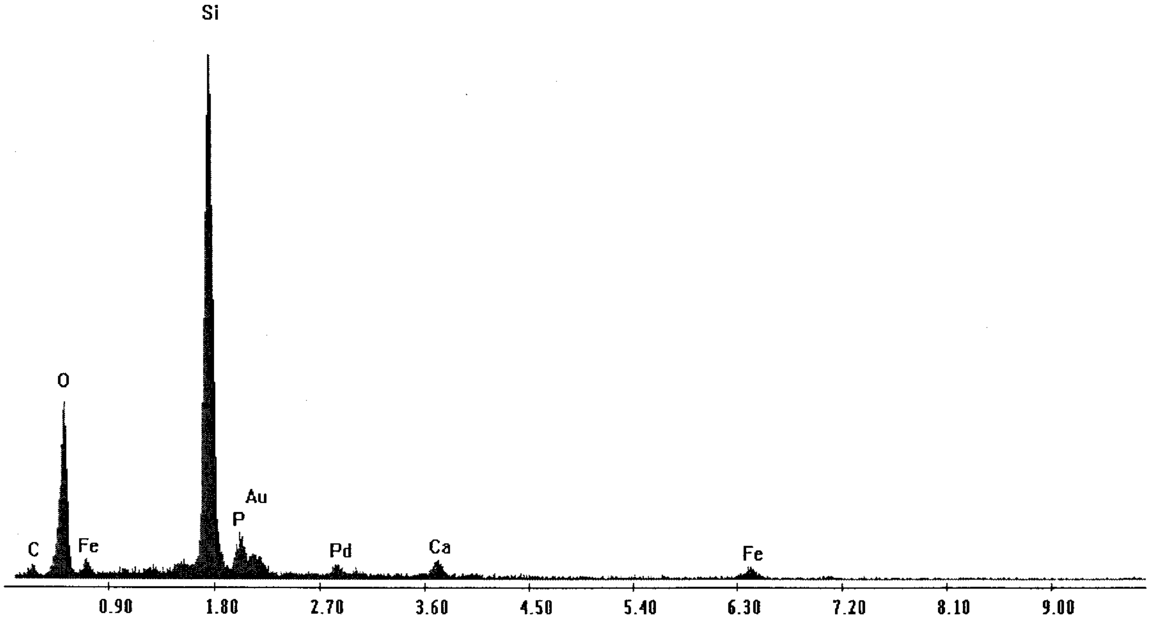

e. Sample B3

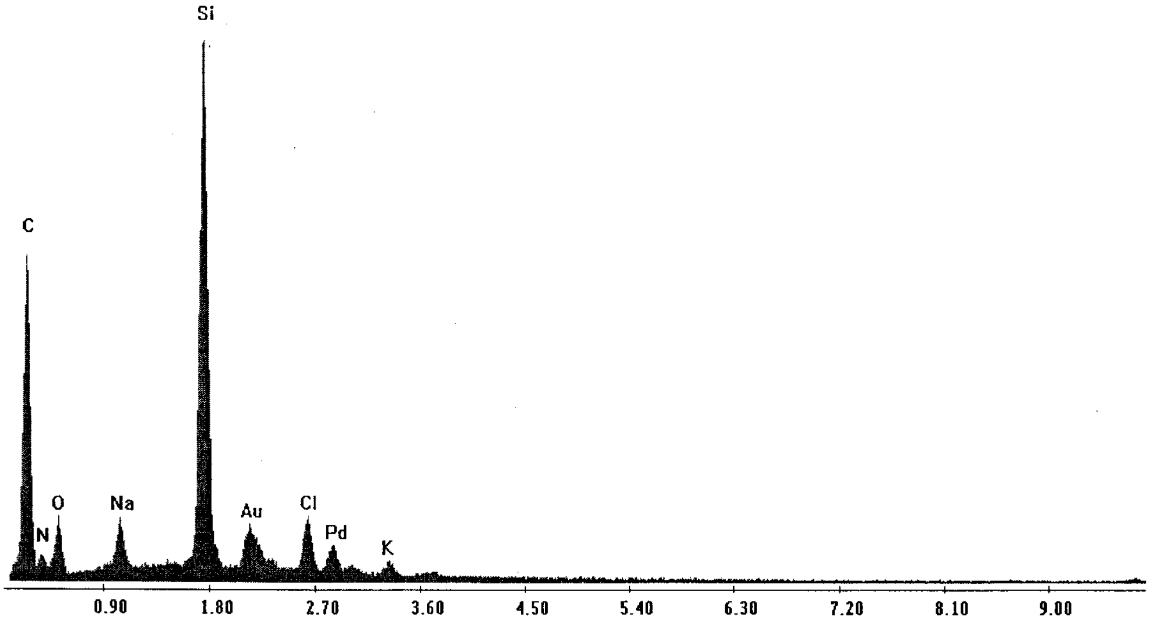

f. Sample C1

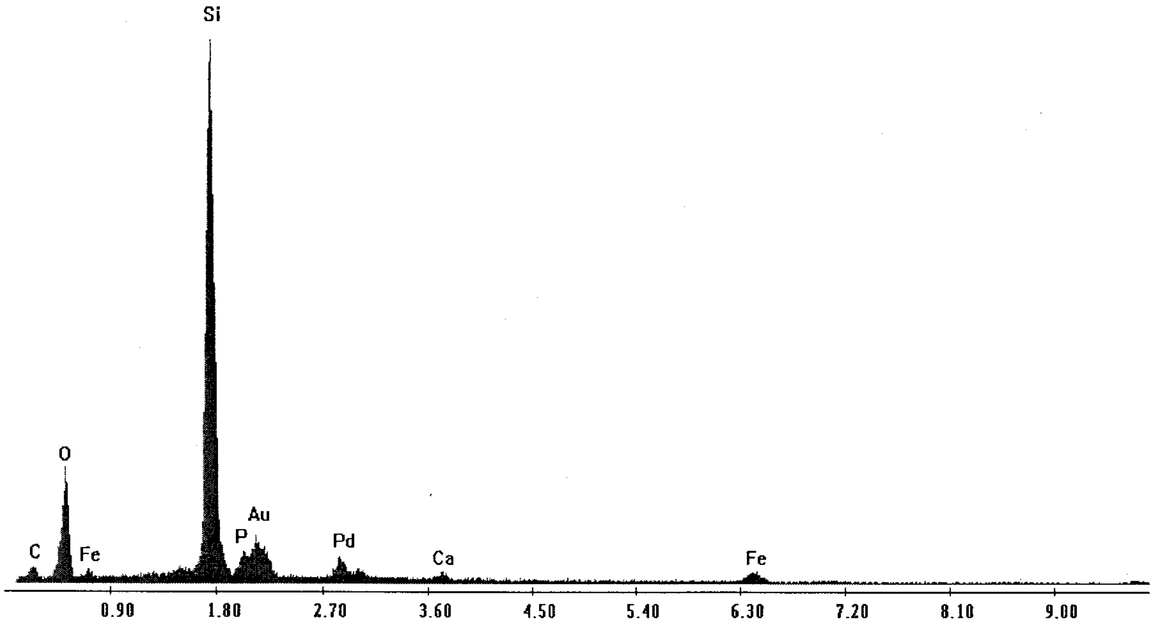

g. Sample C2

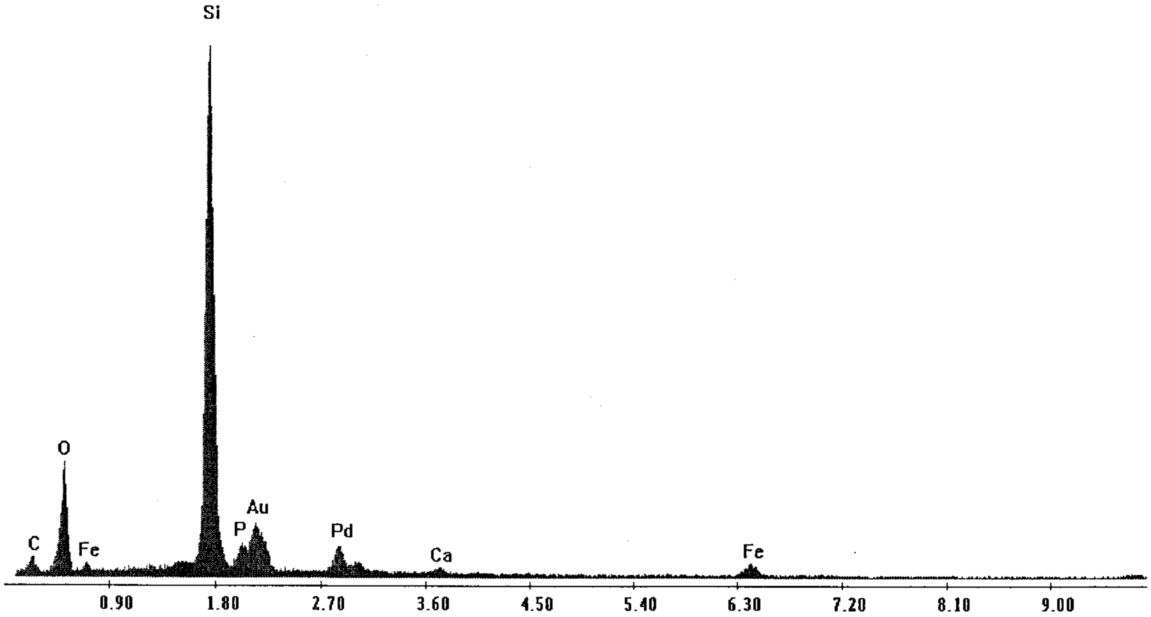

h. Sample C3

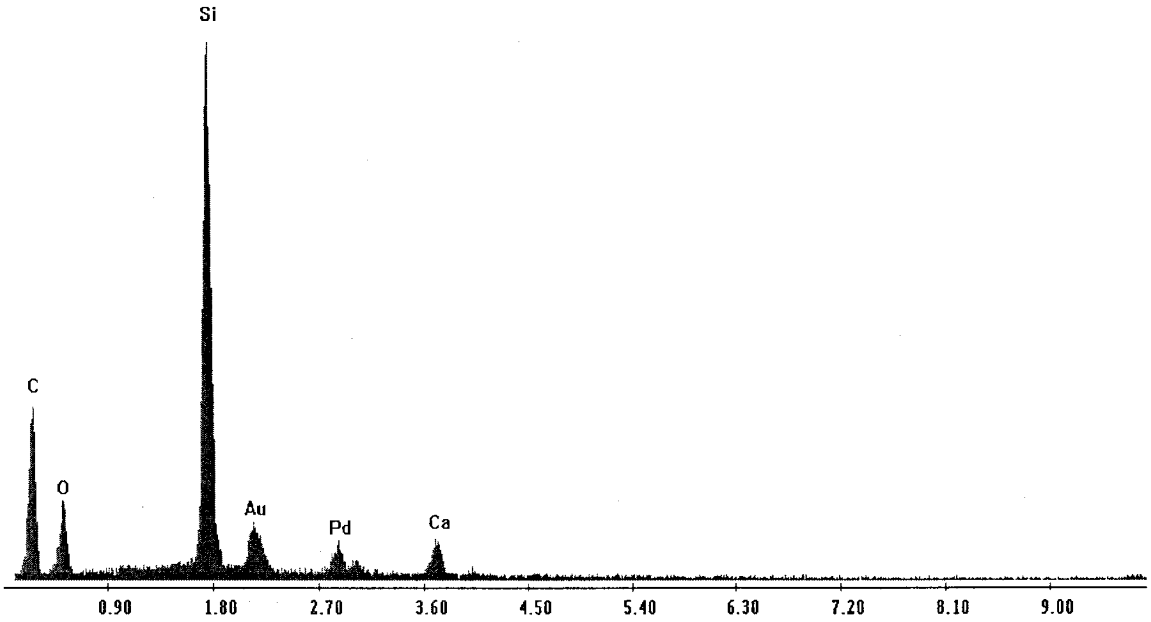

i. Sample D1

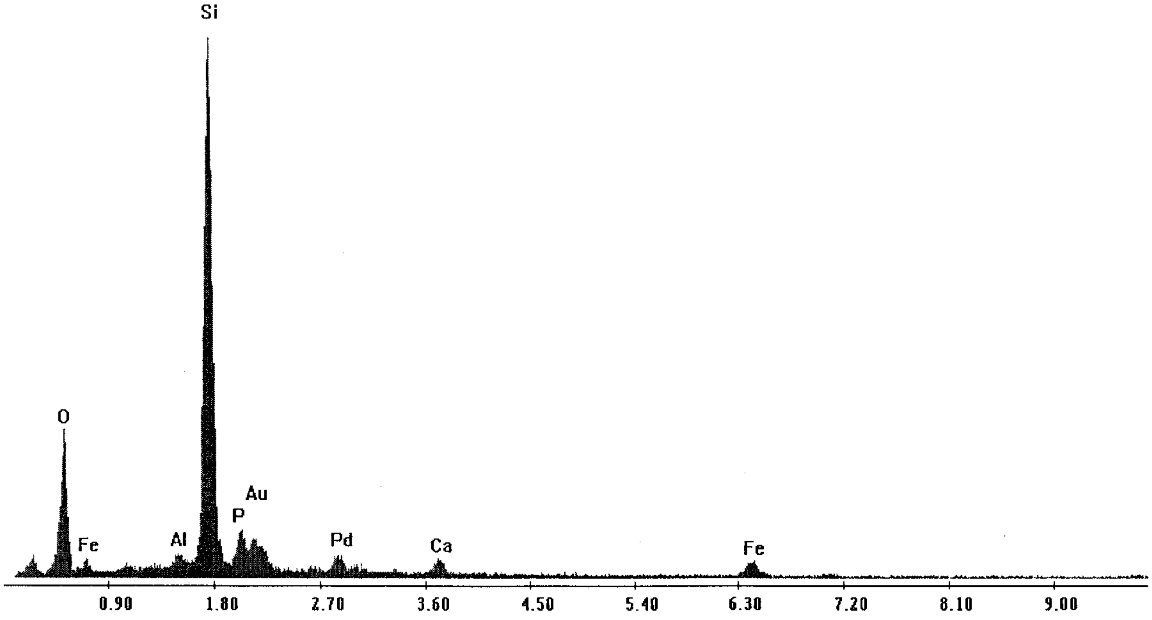

j. Sample D2

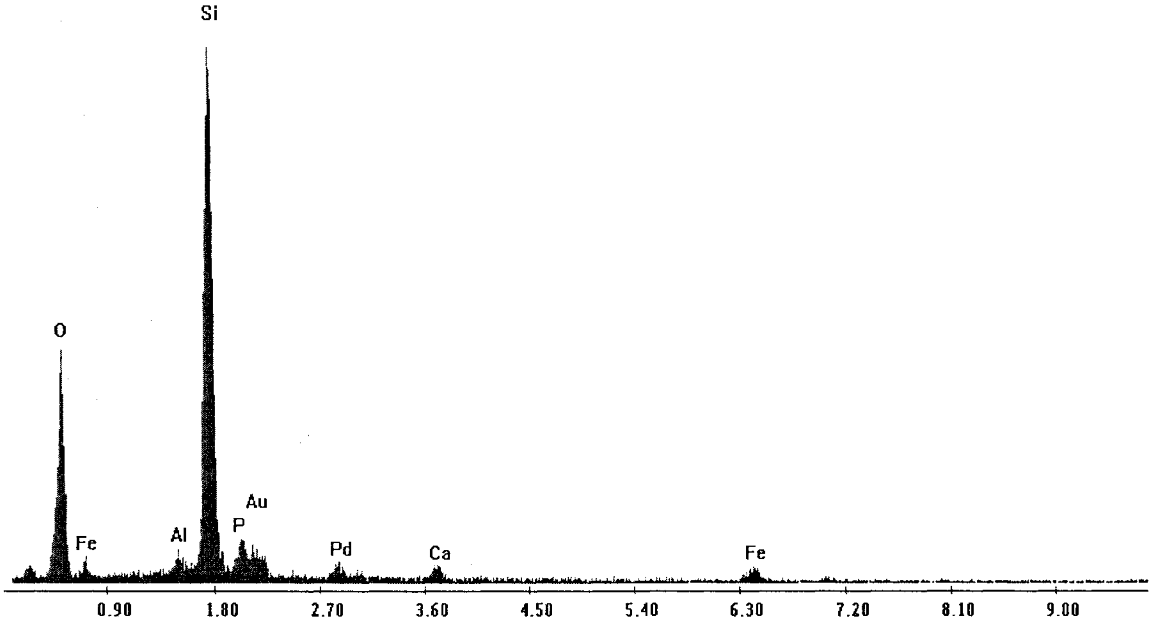

k. Sample D3

Figure 4-5 Composition of the foulants on the sleeves from low pressure UV systems

Figure 4-5 a. shows that there are no fouling materials on the control: silica is the main element of the sleeves; gold and platinum are coated on the samples to achieve electronic conductivity; carbon and oxygen are inherent elements on the sleeves.

Compared with the control, the fraction of carbon increases highly in the permanent foulants on Samples A, B1, and C1 which underwent chemical/mechanical cleaning, and potassium, sodium and chloride appear to be the main fouling elements. But for Sample D1, which also experienced a similar chemical/mechanical cleaning, the carbon fraction increases only slightly, and calcium is the main fouling element while potassium, sodium and chloride are absent. This difference may be attributable to the specific wastewater quality. Interestingly, for all these four samples, the common fouling materials, iron and aluminum, cannot be detected.

In contrast, the foulants on the samples undergoing only mechanical cleaning show similar compositions to those on the samples without any cleaning. For example, the compositions of Samples B2 and B3 (without cleaning) are almost the same: the fraction of carbon is not high, while iron, calcium and phosphorus are the major fouling materials. Samples C2 and C3 (without cleaning) show similar compositions too. Although the compositions of Samples D2 and D3 were similar, they had very different components from other samples: the fraction of iron is much higher than for the other samples, and aluminum is detected. In fact, iron, aluminum, calcium and phosphorus are the main fouling elements on Samples D2 and D3.

- Sleeve samples from medium pressure UV systems

The compositions of the foulants on the sleeves from medium pressure UV systems are shown in Figures 4-6, a ~ g.

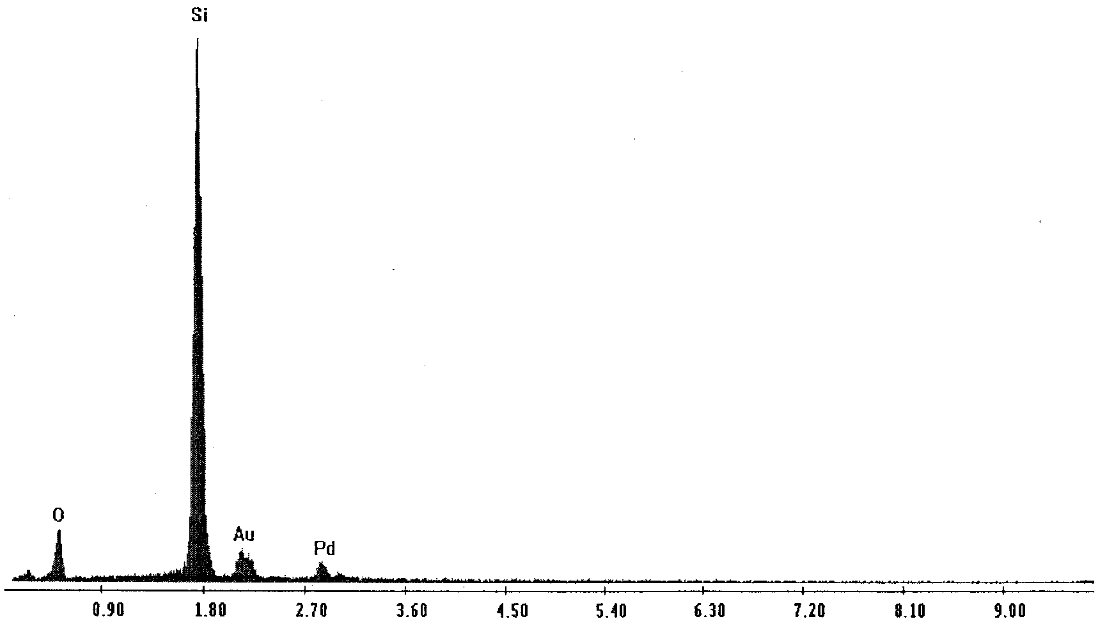

a. Control Medium

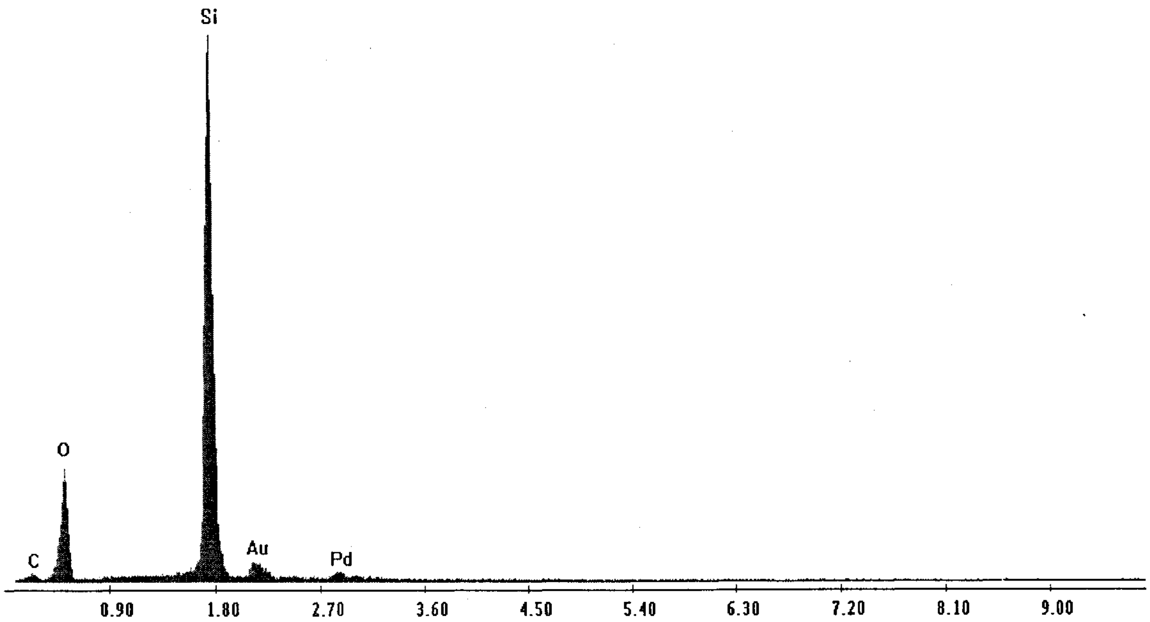

b. Sample X1

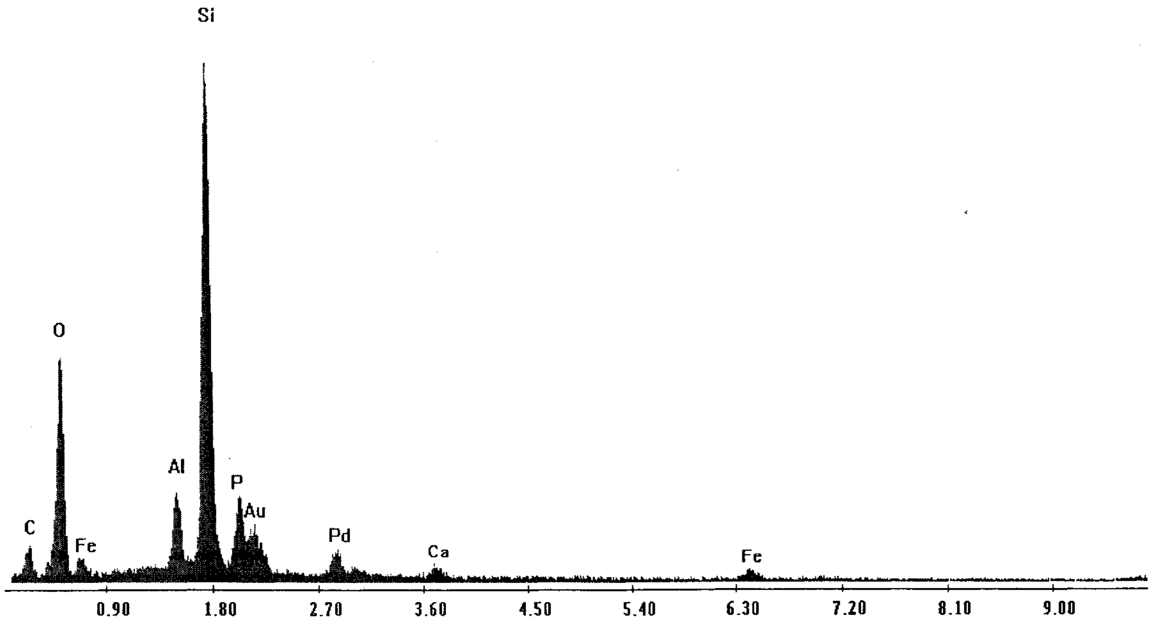

c. Sample X2

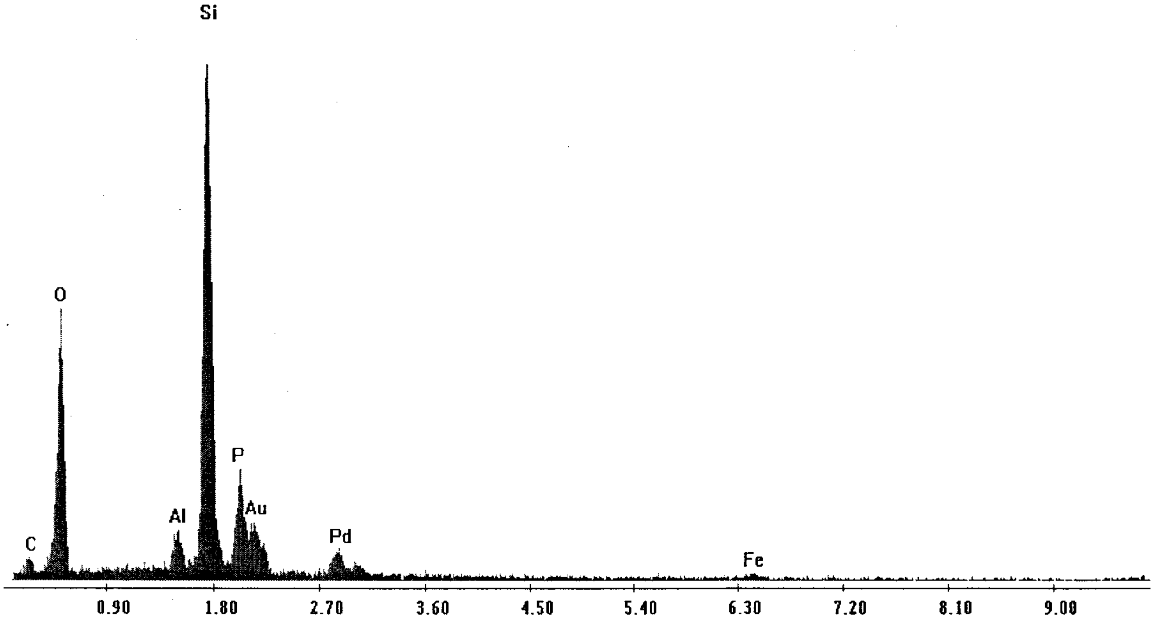

d. Sample Y

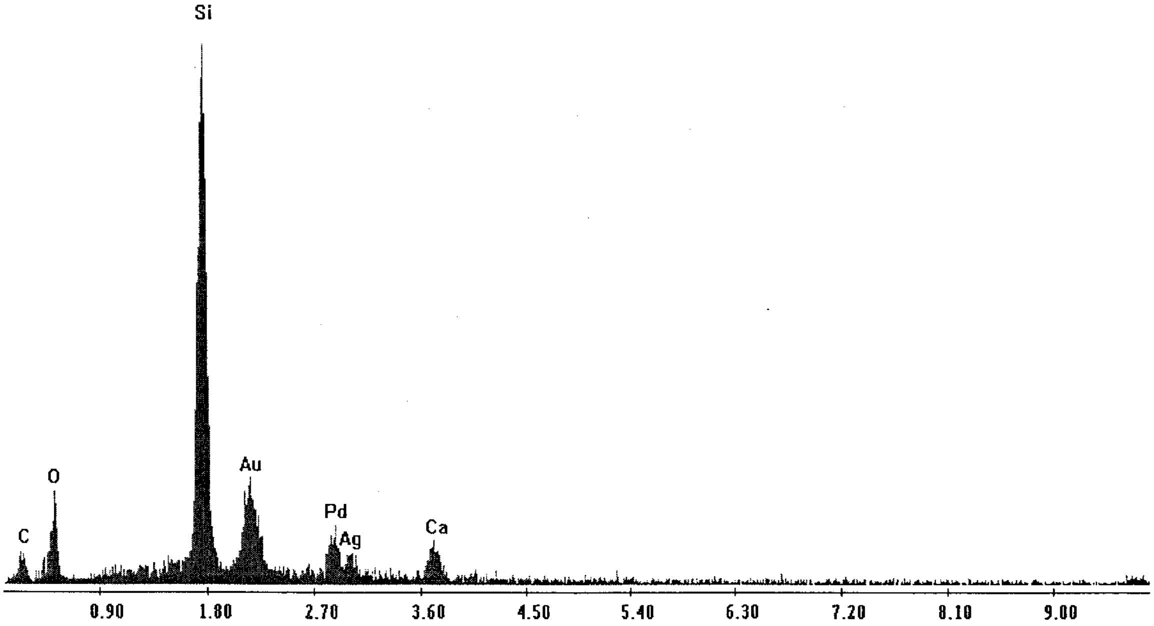

e. Sample Z

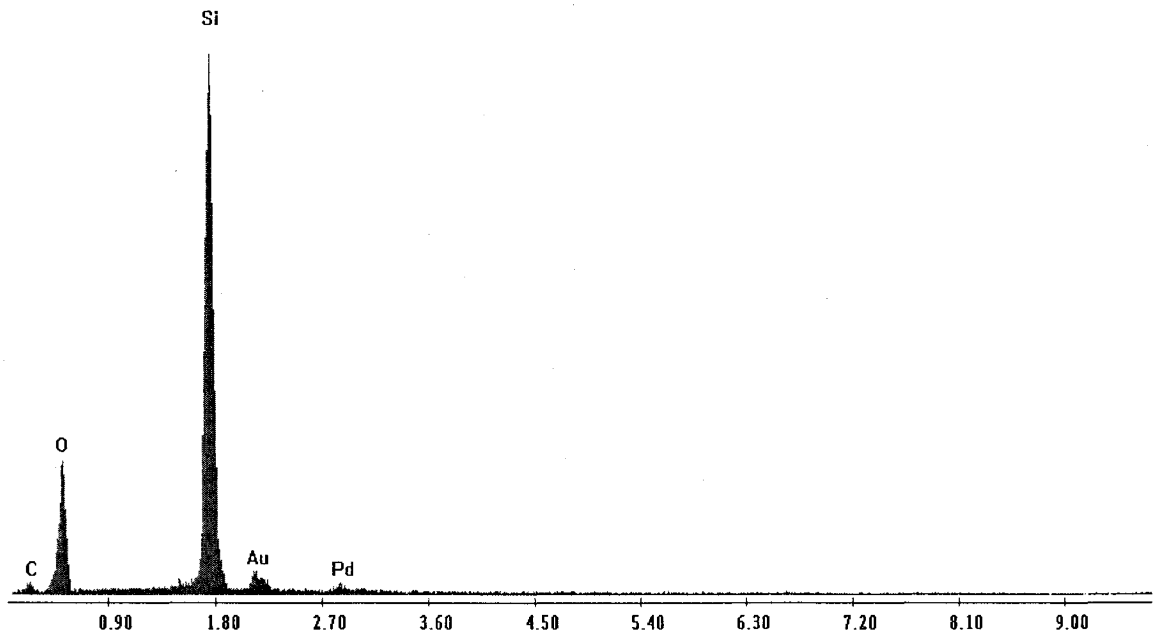

f. Control S

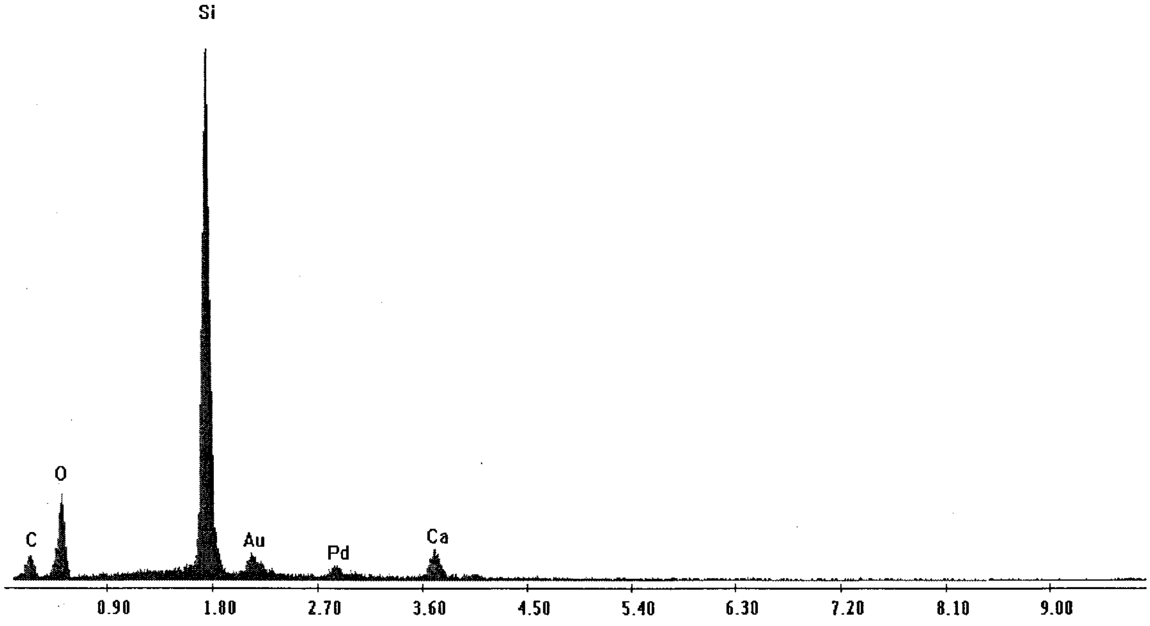

g. Sample S

Figure 4-6 Composition of the foulants on the sleeves from medium pressure UV systems

No common fouling materials (i.e. iron or aluminium) were detected in the foulants on Sample X1. But the foulants on Sample X2 show a high fraction of iron and aluminum, as well as calcium and phosphorus, although Sample X2 came from the same sleeve as Sample X1. On the other hand, there are common fouling materials found on Samples Y and Z. Iron, aluminum, and phosphorus are found to be the major fouling materials on Sample Y, while calcium and silver are the major fouling elements on Sample Z. The only fouling element detected on the surface of Sample S is calcium. The fraction of carbon on all fouled samples is very similar, perhaps because when the medium pressure UV lamps were on, the higher UV intensity would remove most of the organic foulants effectively (Lin, et al., 1999a).

Thus the compositions of the permanent foulants on various samples are very different, and site specific, which may be attributed to the specific wastewater quality. It appears that it is calcium rather than iron and aluminum that can be detected in the permanent foulants more frequently.

4.4 Quantitative Analyses

To determine the weights of various chemicals in the foulants, and to attempt to find a correlation with the wastewater quality, quantitative analyses are necessary. X-ray Fluorescence (XRF) was employed for the quantitative analysis, because it is more sensitive than SEM and can detect even trace elements accurately. Note that, as stated in the Methods section, XRF has detection limits, therefore apparent absence of these metals may simply mean that they are below the detection limits.

- Sleeve samples from low pressure UV systems

The relative mass (%) of the significant chemicals in foulants on the sleeves from low pressure UV systems is listed in Table 4-4.

Table 4-4 Relative mass of significant chemicals in permanent foulants on sleeves from low pressure UV systems

Sample	Al	Fe	Mg	Ca	Na	P	Cl	S	C
Control Low	0.01		0.02	0.03				0.01	
Sample A	0.03	0.01	0.02	0.02					
Sample B1	0.01		0.02	0.02		0.04			
Sample B2	0.45	0.25	0.37	0.71	0.01	**6.16***	0.09	0.22	**1.1**
Sample B3	0.49	0.26	0.39	0.70	0.07	**6.29**	0.03	0.18	**1.27**
Sample C1		0.04	0.02	0.01		0.02			
Sample C2	0.06	0.05	0.04	0.08	0.02	0.48	0.02	0.04	
Sample C3	0.37	0.61	0.19	0.65	0.08	**6.43**	0.03	0.22	**1.82**
Sample D1	0.01		0.02	0.06		0.03		0.02	
Sample D2	0.22	0.09	0.09	0.15	0.07	**1.57**	0.02	0.07	
Sample D3	**1.26**	0.54	0.24	0.76	0.07	**7.57**	0.05	0.28	**1.23**

*: bold numbers means that the mass of a specific chemical is above 1%.

The common fouling materials, such as aluminum, iron, magnesium and calcium were detected on the samples undergoing chemical/mechanical cleaning. Phosphorus and sulfur were the other major fouling elements. Phosphorus was detected on all fouled samples except Sample A. Sulfur could not be found in the permanent foulants on most samples undergoing chemical/mechanical cleaning. Even on Sample D1, the mass of sulfur was insignificant. Carbon is found mainly on the samples without any cleaning.

The components detected by XRF are different from those detected by SEM, as shown in Table 4-5. Chloride detected by XRF is only on the samples experiencing mechanical cleaning or without any cleaning, but it is found by SEM also on the samples undergoing only chemical/mechanical cleaning. In contrast, potassium is detected by SEM in permanent foulants on the samples undergoing only chemical/mechanical cleaning, but it is found by XRF on the samples experiencing mechanical cleaning or without any cleaning. Sodium can be detected by SEM in permanent foulants on the samples undergoing chemical/mechanical cleaning, but cannot be found by XRF on any sample. The high faction of carbon found by SEM on the samples undergoing chemical/mechanical cleaning cannot be detected by XRF. However, this could mean that the mass of these undetected elements is below the detection limit of XRF.

Table 4-5 Comparisons of detection results between SEM and XRF

Sample	Al	Fe	Mg	Ca	Na	K	P	Cl	S	C
Sample A	x*	x	x	x	s	s		s		s
Sample B1	x		x	x	s	s	x	s		s
Sample B2	x	x,s	x	x,s	x		x	x	x	x,s
Sample B3	x	x,s	x	x,s	x		x,s	x	x	x,s
Sample C1		x	x	x	s	s	x	s		x,s
Sample C2	x	x,s	x	x,s	x		x,s	x	x	s
Sample C3	x	x,s	x	x,s	x	x	x,s	x	x	x,s
Sample D1	x		x	x,s			x		x	s
Sample D2	x,s	x,s	x	x,s	x		x,s	x	x	
Sample D3	x,s	x,s	x	x,s	x		x,s	x	x	x

*: x and s mean that this chemical is detected by XRF or SEM, respectively.

The reasons for this inconsistency are not clear. Some elements, such as magnesium, aluminum and iron, were not detected by SEM, but were detected by XRF because of its better sensitivity. But some other elements, such as chloride, potassium and sodium, were found by SEM, but not by XRF. Possible explanations are: (1) SEM and XRF detected different foulants on the same sample. There were many foulants on one sample, so it was impossible for SEM and XRF to detect the same specific foulants. (2) SEM and XRF have their own limits and errors in use.

Thus, to accurately determine the composition of permanent foulants, the results from SEM and XRF should be combined to avoid errors and increase the reliability. Based on the integrated analyses, the main fouling components in the permanent foulants tested herein were aluminum, iron, magnesium, calcium, and phosphorus. It is difficult to decide which are the major elements because of their approximate mass, which may be decided by wastewater quality. Potassium, sodium, carbon and chloride were also found in the permanent foulant.

- Sleeve samples from medium pressure UV systems

The relative mass (%) of the main chemicals in foulants on the sleeves from medium pressure UV systems is listed in Table 4-6.

Table 4-6 Relative mass of major chemicals in permanent foulants on sleeves from medium pressure UV systems

Sample	Al	Fe	Mg	Ca	Na	P	Cl	S	C
Control Medium			0.02						
Sample X1		0.04	0.02						
Sample X2	**5.81**	0.47	0.24	0.58	0.04	**12.52**	0.01	0.06	**1.93**
Sample Y	**1.97**	0.08	0.09	0.20	0.08	**3.93**	0.01		**1.35**
Sample Z									0.56
Control S	< 0.01		< 0.01			< 0.01		< 0.01	
Sample S	0.02		0.06			0.04		0.01	

Sample X2 underwent only mechanical cleaning and it has a higher mass of fouling elements than the other samples. For Sample X1, iron and magnesium were detected by XRF. For Sample Z, only a high mass of carbon was found, while calcium which was detected by SEM, was absent here. There were many types of fouling materials in Sample Y. Aluminum and phosphorus were the major fouling elements, but iron, magnesium, and calcium were also important. For Sample S, magnesium and phosphorus were the major fouling elements in the permanent foulants. Aluminum was also detected, but iron was not present. Trace quantities of sulfur were detected.

Unlike the permanent foulants on the sleeves from low pressure UV systems, there were no common fouling elements in the permanent foulants on the sleeves from medium pressure UV systems. The components were very site specific. Since Sample Y has a higher mass of fouling materials, and the mechanical cleaning did not damage the sleeve surface severely (the roughness of the sample is satisfactory), it can be assumed that the wastewater quality itself at System Y is responsible for the higher mass of the fouling elements.

In general, iron, aluminum, calcium, magnesium and phosphorus compose the majority of the elements in the permanent foulants. However, the compositions of the permanent foulants are variable, and site specific.

4.5 Wastewater Quality Analyses

4.5.1 General

The composition and mass of the chemicals in the permanent foulants were shown to be site specific. Similarly, the fouling rates, which affect the SUVT of the sleeves undergoing chemical/mechanical cleaning and the intervals of chemical/mechanical cleaning, differ for different UV disinfection systems. An attempt was made to correlate these variations with the wastewater quality at different sites. The average wastewater quality in the low pressure UV systems is listed in Table 4-7.

Table 4-7 Wastewater quality in low pressure UV systems (2000, 2001)

System	System A	System B	System C	System D
Chemical added (for coagulation)	Alum	N/A	$FeCl_3$	Alum
pH	7.2	7.5	7.3	7.3
TSS (mg/L)	20	N/A	8	5
Turbidity (NTU)	6	0.42	N/A	1.22
Alkalinity (mg/L)	100	288	145	177
Temperature (^0C)	14-25	17-26	15-25	14-25
TOC (mg/L)	6.2	4	N/A	4.3
Hardness as $CaCO_3$ (mg/L)	209	453	225	279
Aluminum Al (mg/L)	0.82	0.04	0.06	0.38
Iron Fe (mg/L)	0.07	0.08	0.35	0.13
Calcium Ca (mg/L)	62.6	120	69	75.7
Magnesium Mg (mg/L)	12.4	37	16.2	16.6
Potassium K (mg/L)	10.5	11.5	10.7	10.2
Sodium Na (mg/L)	73.6	190	173	109
Phosphorus P (mg/L)	1.1	3	0.89	0.5
Fouling rate (% loss of SUVT/ day)	2.1	3.3	9.9	9.4

N/A = data not available

From Table 4-7, it is difficult to determine the affect of TSS (total suspended solids) and turbidity on permanent fouling. System A had the highest concentration of TSS, however Sample A possessed the highest SUVT (99.05%) and lowest fouling rate (2.1 % loss of

SUVT/day). TSS did not increase the amount of permanent foulants in System A. And although Systems C and D had low concentrations of TSS, they also had the lowest SUVT. Hence there appears to be no relationship between the concentration of TSS and SUVT. Similarly, the high turbidity in System A did not appear to increase permanent fouling, and System D had the highest mass of permanent fouling even though it had the lowest turbidity. Only in System B, the low turbidity was associated with high SUVT, low fouling rate and low permanent fouling.

Figure 4-7 shows Alkalinity and Hardness in these four systems.

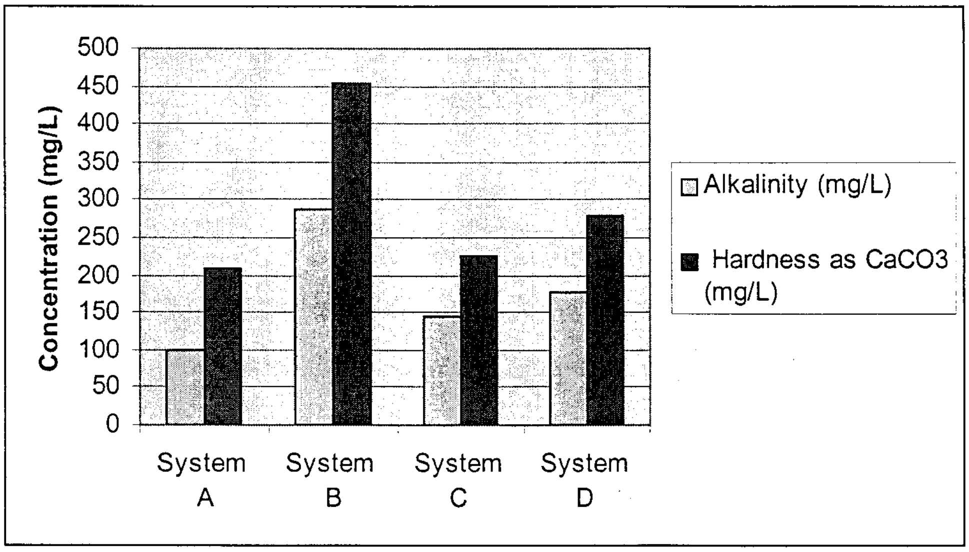

Figure 4-7 Alkalinity and hardness in Systems A, B, C, and D

It can be seen that the alkalinity varied with the hardness (as expected). Sehnaoui (2001) showed that the hardness was almost always elevated in systems with high fouling rates. Systems A, C, and D verified this conclusion. Systems C and D had higher fouling rates than System A, and there was higher hardness in Systems C and D than in System A. However, for System B, although it had a lower fouling rate, its hardness was the highest among these four systems.

The influence of TOC (total organic carbon) on the permanent fouling was also unclear. System A had the highest TOC and SUVT, but the lowest fouling rate. On the other hand, although Systems B and D had similar concentrations of TOC, the SUVT of their sleeves and the fouling rates were very different.

Figure 4-8 shows the relationship between the concentrations (mg/L) of aluminum in the wastewater of four systems and its mass (%) in permanent foulants on Samples A, B1, C1, and D1.

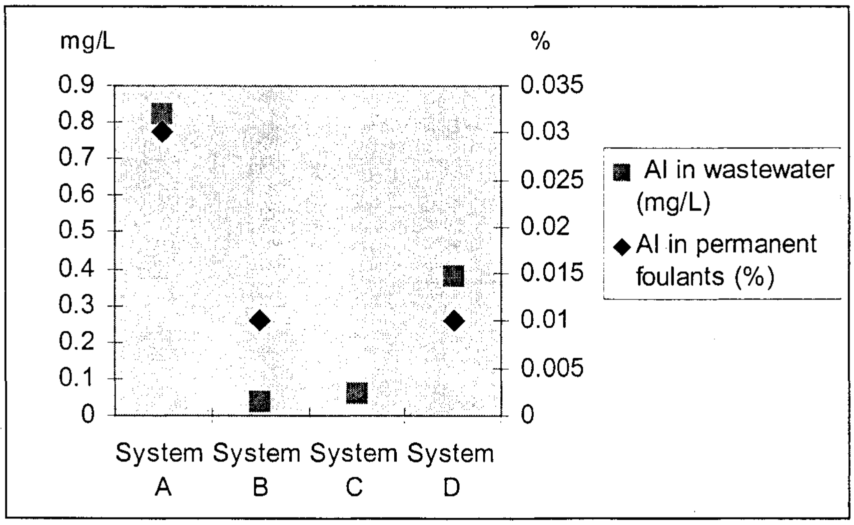

Figure 4-8 Concentrations of aluminum in the wastewater and relative mass of aluminum in permanent foulants

Alum was added to Systems A and D, so there were higher concentrations of aluminum in these two systems than in the other two systems. As a result, the high concentration of aluminum in System A led to the highest mass of Al in the permanent foulants on Sample A. Moreover, there was a low concentration of aluminum in Systems C and D, so that no aluminum was detected in the permanent foulants on Sample C1, and the mass of aluminum in the permanent foulants on Sample D1 was just at the detection limit of the XRF (0.01%). However, there was only a tiny mass of aluminum in the permanent foulants on Sample D1, although System D had a high concentration of aluminum in the wastewater. Thus, the concentration of aluminum in the wastewater showed some influence on the mass of aluminum in the permanent foulants, but it was not the sole factor.

Figure 4-9 shows the relationship between the concentrations (mg/L) of iron in the wastewater and its mass (%) in permanent foulants in these four systems.

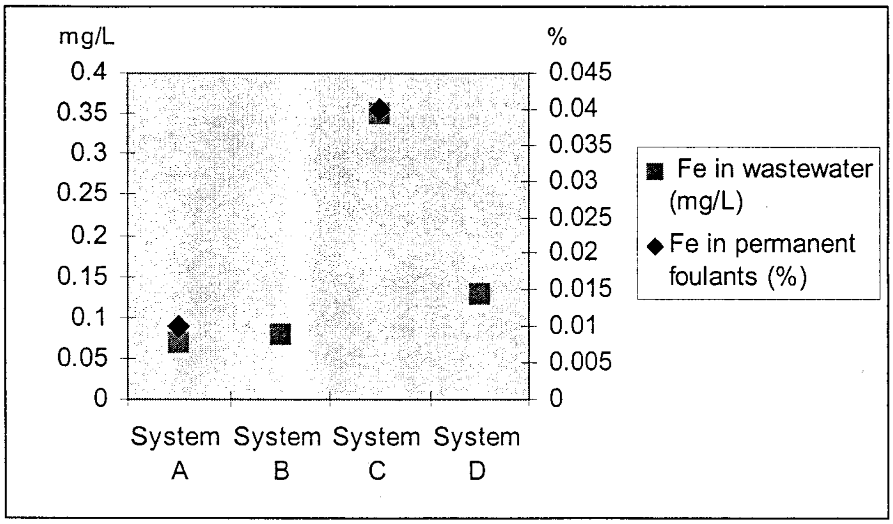

Figure 4-9 Concentrations of iron in the wastewater and relative mass of iron in permanent foulants

Ferric chloride was added to System C. Therefore, the highest concentration of iron was in the wastewater of System C and the highest mass of iron was in the permanent foulants on Sample C1. The concentration of iron in Systems A, B, and D was lower and similar, and no was iron detected in the permanent foulants on Samples B1 and D1. Although iron was found in the permanent foulant on Sample A, the mass was tiny, just at the detection limit of the XRF (0.01%). It is possible therefore that a higher concentration of iron in the wastewater could affect the mass of iron in the permanent foulants.

It was difficult to determine the effects of calcium, magnesium and phosphorus. System B had the highest concentration of calcium in the wastewater, but a low mass in the permanent foulants. System D had a lower concentration of calcium, but the highest mass of calcium in the permanent foulants. Furthermore, the concentrations of magnesium in the wastewater of all four systems were very different, but there was approximately the same mass in the permanent foulants on all sleeve samples. Moreover, the concentration of phosphorus in System A was higher than that in System D, but there was no phosphorus detected in the permanent foulants on Sample A.

Although potassium and sodium were abundant in all four systems, and were found by SEM in the permanent foulants, their mass in the permanent foulants was below the detection limit of XRF. Hence, the high concentrations of potassium and sodium in the wastewater had almost no influence on the mass in the permanent foulants.

Wastewater quality (average value) in the medium pressure UV systems is listed in Table 4-8.

Table 4-8 Wastewater quality in medium pressure UV systems (2001)

System	System X	System Y	System Z	System S
Chemical added (for coagulation)	Alum	N/A	$FeCl_3$	Alum, Polymer
pH	7.38	6.91	7.13	7.2
Turbidity (NTU)	1.83	45.8	5.01	
Alkalinity (mg/L)	180	176	172	
TOC (mg/L)	4.44	8.45	8.1	
Hardness as $CaCO_3$ (mg/L)	240	366	194	
Aluminum Al (mg/L)	0.22	0.94	0.07	0.05
Iron Fe (mg/L)	0.03	5.08	0.6	
Calcium Ca (mg/L)	73.5	114	59.2	
Magnesium Mg (mg/L)	13.7	19.9	11.1	
Potassium K (mg/L)	6.8	7.83	7.48	
Sodium Na (mg/L)	70	108.	66.6	
Phosphorus P (mg/L)	0.72	5.13	0.48	
TSS (mg/L)				20
BOD (mg/L)				17.5
COD (mg/L)				70

The effects of turbidity and hardness are apparent here. Since System Y had the highest turbidity and hardness in the wastewater, it also had the highest fouling rate and the lowest SUVT of the sleeves. However, unlike the low pressure UV systems, the alkalinity here was similar in all three systems, and was not consistent with the hardness. Thus, the effect of alkalinity was not clear. Moreover, it was also difficult to assess the influence of TOC, because although Systems Y and Z had similar concentrations of TOC, they had very different fouling rates but similar (satisfactory) SUVT.

Although no chemicals were added to System Y, it had a higher concentration of aluminum in the wastewater than did System X, into which alum was added. As a result, only on Sample Y was aluminum detected by XRF. Similarly, System Y had a higher concentration of iron in the wastewater than System Z into which ferric chloride was added. Thus, no iron was detected on Sample Z, but a high mass of iron was found on Sample Y. Moreover, although System X had the lowest concentration of iron in the wastewater, a significant mass of iron was detected on Sample X1.

The effects of calcium and magnesium were obvious. System Y had the highest concentrations of calcium and magnesium, thus it also had the highest mass of these two elements on Sample Y. System X had a higher concentration of magnesium in the wastewater than System Z, so a higher mass of magnesium was detected in the permanent foulants on Sample X1. On the other hand, the influence of potassium and sodium were almost negligible.

System Y had the highest concentration of phosphorus in the wastewater; this explains why only on Sample Y was phosphorus detected.

In general, the effect of wastewater quality on the permanent foulants in medium pressure UV systems was more apparent than that in low pressure UV systems.

Only a few parameters were measured in System S. Because of the lack of data, it was difficult to assess the affect of the wastewater quality in System S. However, it was reasonable that aluminum was detected in the permanent foulants on Sample S since alum was added into the wastewater. Although System S used polymer for coagulation, TSS was still high, which indicated that the effects of polymer were not apparent. Furthermore, because the wastewater quality in System S was quite good (BOD was low, and COD and TSS were medium), but the sleeves only had the moderate SUVT (93.6%), it may be claimed that it was not the wastewater quality that reduced the SUVT in System S. Based on this study, a reasonable explanation is that it is the damage on the sleeves caused by the mechanical cleaning that reduces the UV transmittance by trapping more permanent foulant.

4.5.2 Correlations

In this study, a mathematical correlation between wastewater quality and permanent fouling (including chemical composition, fouling rates and SUVT) was performed. Unfortunately, there were insufficient data for wastewater quality available. Although some correlation coefficients were calculated, and they can lead to some conclusions, they were not really convincing because of the lack of data. For example, in the four low pressure UV systems, some specific parameters (average value) of wastewater quality were measured in three systems but not in the fourth. When calculating the correlation coefficient between this parameter and the fouling rate or SUVT, only three data points for two variables could be used. Thus, the final correlation coefficients are not robust. Nevertheless, the correlation coefficients are still given so that they can act as a guide for further research.

- Correlation coefficients for low pressure UV systems are listed in Table 4-9.

Table 4-9 Correlation coefficients for low pressure UV systems

Correlation	Correlation coefficient
TSS (mg/L) vs. SUVT (%)	**0.9999***
Turbidity (NTU) vs. SUVT (%)	**0.71**
Alkalinity (mg/L) vs. SUVT (%)	-0.16
TOC (mg/L) vs. SUVT (%)	**0.71**
Hardness as $CaCO_3$ (mg/L) vs. SUVT (%)	0.01
TSS (mg/L) vs. fouling rate	**-0.97**
Turbidity (NTU) vs. fouling rate	**-0.52**
Alkalinity (mg/L) vs. fouling rate	-0.13
TOC (mg/L) vs. fouling rate	**-0.52**
Hardness as $CaCO_3$ (mg/L) vs. fouling rate	-0.31
TSS (mg/L) vs. roughness (nm)	**-0.91**
Turbidity (NTU) vs. roughness (nm)	**-0.66**
Alkalinity (mg/L) vs. roughness (nm)	0.23
TOC (mg/L) vs. roughness (nm)	**-0.67**
Hardness as $CaCO_3$ (mg/L) vs. roughness (nm)	0.1
Al in wastewater (mg/L) vs. Al in permanent foulants (%)	**0.9**
Fe in wastewater (mg/L) vs. Fe in permanent foulants (%)	N/A
Ca in wastewater (mg/L) vs. Ca in permanent foulants (%)	-0.07
Mg in wastewater (mg/L) vs. Mg in permanent foulants (%)	N/A
P in wastewater (mg/L) vs. P in permanent foulants (%)	**0.78**

*: bold numbers show that these correlation coefficients are in the range from ±0.5 to ±1, which means that the two variables have a relatively close correlation.

From Table 4-9, it can be seen that TSS, Turbidity and TOC have a relatively close relationship to permanent fouling which is represented by SUVT, fouling rate and roughness, because all the correlation coefficients are in the range from ±0.5 to ±1. The influence of TSS is most obvious. It is worth noting that TSS, Turbidity and TOC representing wastewater quality show a positive relation to SUVT, and a negative relation to fouling rates and roughness, because there is a nearly inverse relationship between SUVT and fouling rates or roughness which is discussed in the previous sections. This relationship is also shown in Figures 4-10 a~b. From the figure, it also can be seen that the relationship between SUVT and fouling rates or roughness is approximately linear (the straight line in each diagram is the trendline). Thus, SUVT, fouling rate and roughness can be considered together. SUVT can act as a representative of the combination of these three parameters that represents permanent fouling, which is affected most strongly by TSS; Turbidity and TOC also exert influences on it at somewhat weaker levels.

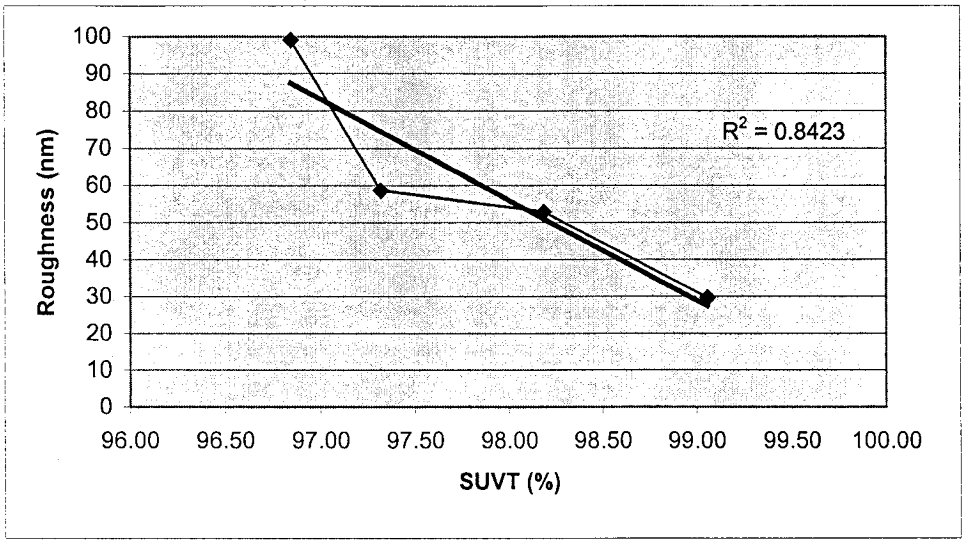

a. SUVT vs. roughness

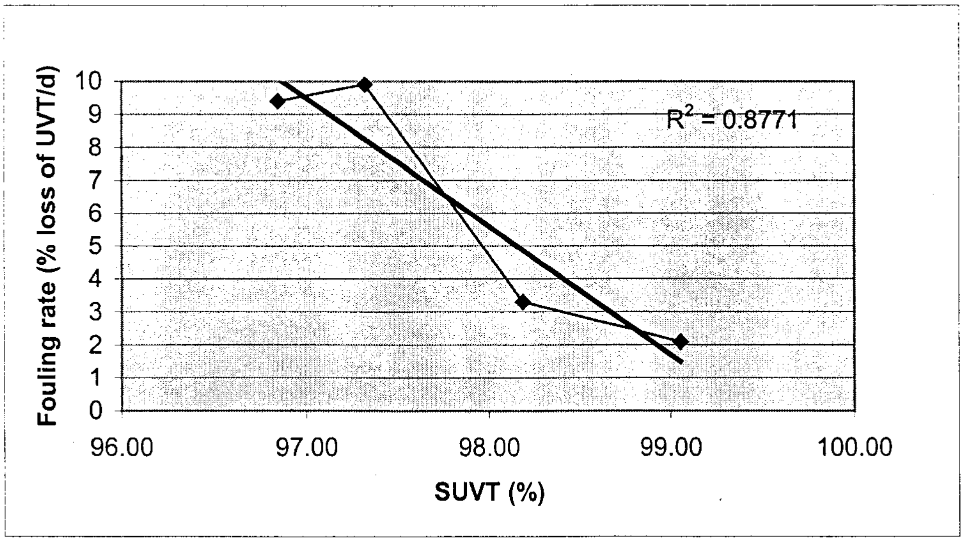

b. SUVT vs. fouling rate

Figure 4-10 Relationship between SUVT and roughness or fouling rate in low pressure UV systems

Since wastewater quality is mainly represented by TSS, Turbidity and TOC, an attempt was made to combine these three parameters into one term. Unfortunately, a value for TSS was absent in System B, and System C had no data on Turbidity and TOC, so it was impossible to determine the mathematical relationship between TSS and Turbidity or TOC. However, the data for Turbidity and TOC in Systems A, B, and D showed that there was a linear relationship between these two parameters, which is displayed in Figure 4-11. Hence Turbidity and TOC can be treated as one term.

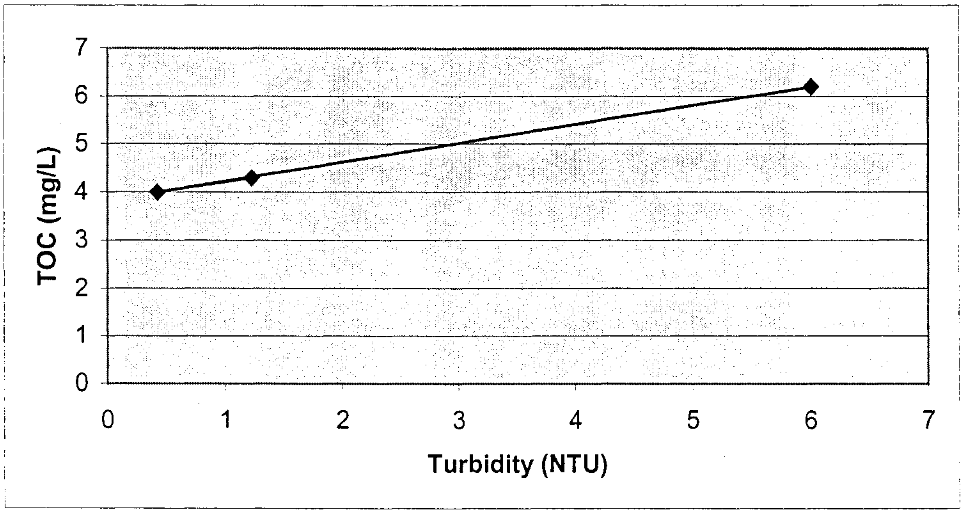

Figure 4-11 Relationship between turbidity and TOC in low pressure UV systems

Because SUVT can represent the combination of SUVT, fouling rates and roughness, and this combination stands for permanent fouling, SUVT is the representative of permanent fouling. Additionally, TSS or the combination of Turbidity and TOC are the representatives of wastewater quality. Then, the mathematical relationship between wastewater quality and permanent fouling, is in fact the relationship between SUVT and TSS or Turbidity (on behalf of the combination of Turbidity and TOC). These two relationships are shown in Figures 4-12 a~b.

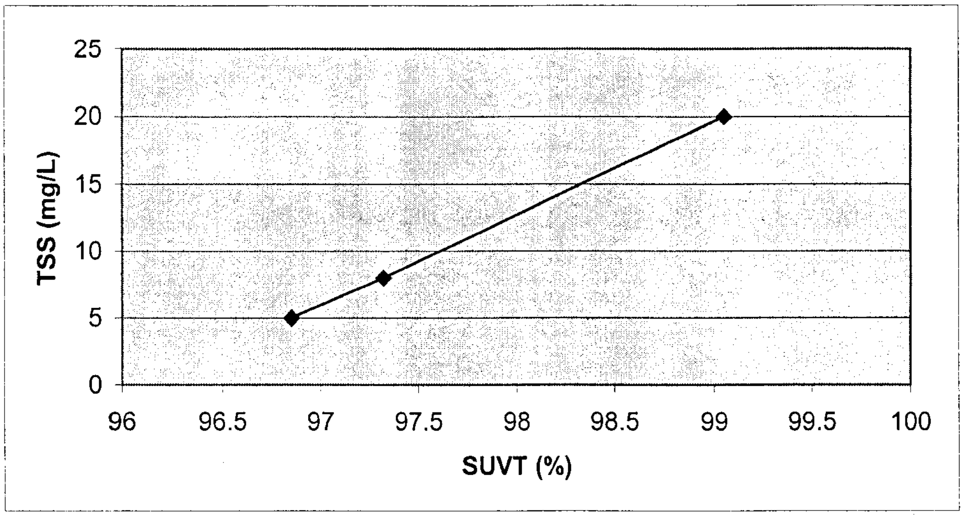

a. SUVT vs. TSS

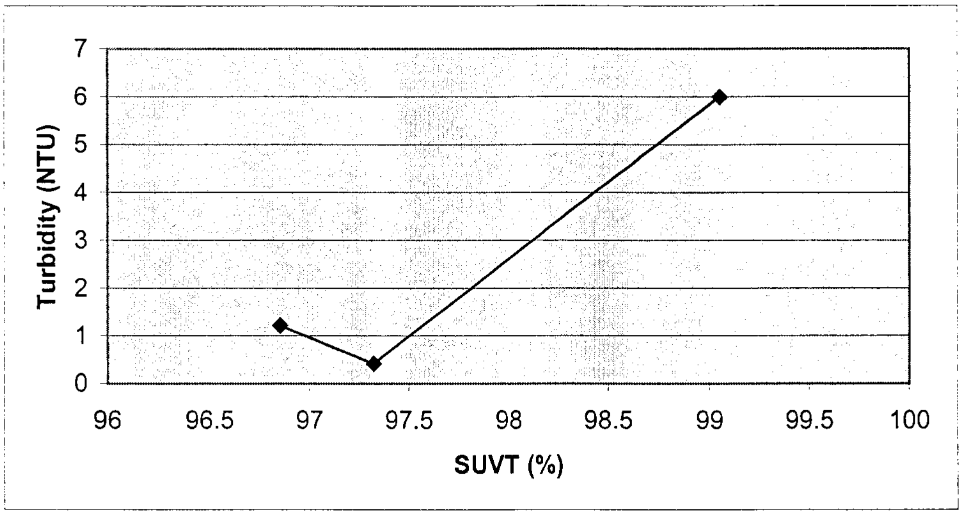

b. SUVT vs. Turbidity

Figure 4-12 Relationship between SUVT and TSS or turbidity in low pressure UV systems

Figure 4-12 a. shows that TSS has a linear relationship to SUVT. This means that a change of TSS will exert an apparent influence on SUVT, which is in agreement with the high correlation coefficient (0.9999) between these two variables. On the other hand, the relationship between SUVT and Turbidity is not clear in Figure 4-12 b. Thus, although the correlation coefficients show that there is a close correlation between permanent fouling and Turbidity or TOC, the effect of the combination of Turbidity and TOC on permanent fouling cannot be established.

For specific components of the permanent foulants, the concentrations of aluminum and phosphorus in the wastewater show a reasonably strong relationship (correlation coefficient > 0.7) to the mass of these two chemicals in the permanent foulants. The affect of the concentration of calcium is insignificant. Because of the lack of data, the correlation coefficients between the concentrations of iron and magnesium in wastewater and the mass of these two elements in the permanent foulants cannot be assessed.

As can be seen from Table 4-9, the affects of alkalinity and hardness were negligible.

- Correlation coefficients in medium pressure UV systems (System S is not included, since no correlation coefficient can be obtained for System S because of the lack of data) are listed in Table 4-10.

Table 4-10 Correlation coefficients for medium pressure UV systems

Correlation	Correlation coefficient
Turbidity (NTU) vs. SUVT (%)	**-0.84**
Alkalinity (mg/L) vs. SUVT (%)	**0.54**
TOC (mg/L) vs. SUVT (%)	**-0.95**
Hardness as $CaCO_3$ (mg/L) vs. SUVT (%)	**-0.62**
Turbidity (NTU) vs. fouling rate	**0.9885**
Alkalinity (mg/L) vs. fouling rate	-0.15
TOC (mg/L) vs. fouling rate	**0.73**
Hardness as $CaCO_3$ (mg/L) vs. fouling rate	**0.89**
Turbidity (NTU) vs. roughness (nm)	**0.78**
Alkalinity (mg/L) vs. roughness (nm)	**-0.63**
TOC (mg/L) vs. roughness (nm)	**0.97**
Hardness as $CaCO_3$ (mg/L) vs. roughness (nm)	**0.54**

Table 4-10 shows that wastewater quality represented by Turbidity, Alkalinity, TOC and Hardness has an obvious relation to permanent fouling represented by SUVT, fouling rate and roughness. However, the affects of different specific parameters of wastewater quality are varied. For example, SUVT and roughness show closer relations to TOC than to other parameters, and fouling rate is affected most intensely by Turbidity. From Figures 4-13 a~b, it can be seen that there is also an inverse relationship between SUVT and fouling rate or roughness in medium pressure UV systems. Hence, the combination of these three items can act as one parameter representing permanent fouling. However, because of the lack of data, the correlation coefficients between the concentrations of fouling materials in the wastewater and the mass of these elements in the permanent foulants cannot be calculated.

Moreover, as can be seen from the table, all the correlation coefficients except one are in the range from ±0.5 to ±1, which verifies again that the effect of wastewater quality on permanent foulants in medium pressure UV systems was more apparent than that in low pressure UV systems.

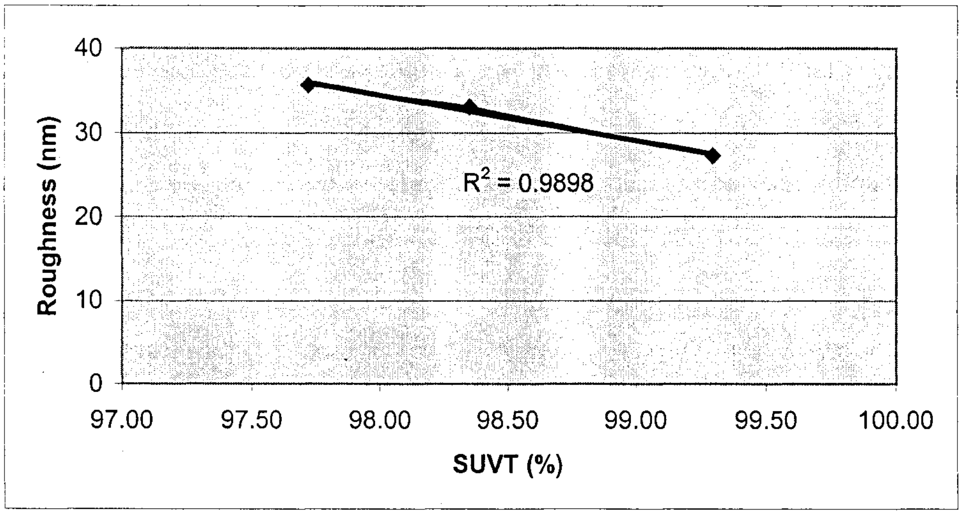

a. SUVT vs. roughness

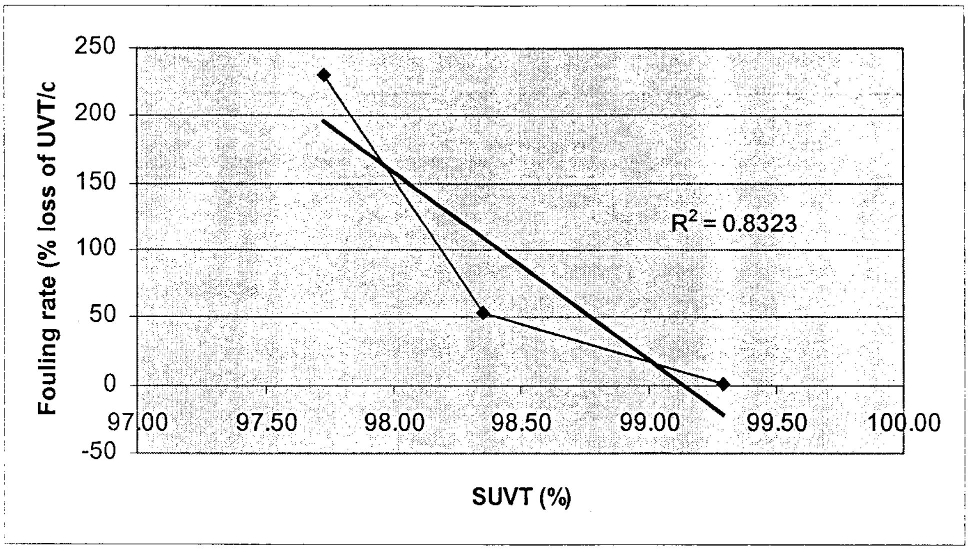

b. SUVT vs. fouling rate

Figure 4-13 Relationship between SUVT and roughness or fouling rate in medium pressure UV systems

Attempts at combining several parameters of wastewater quality into one term failed, because the achieved relationship was not regular and clear. For example, Figure 4-14 shows the relationship between Turbidity and Alkalinity in three medium pressure systems (X, Y and Z).

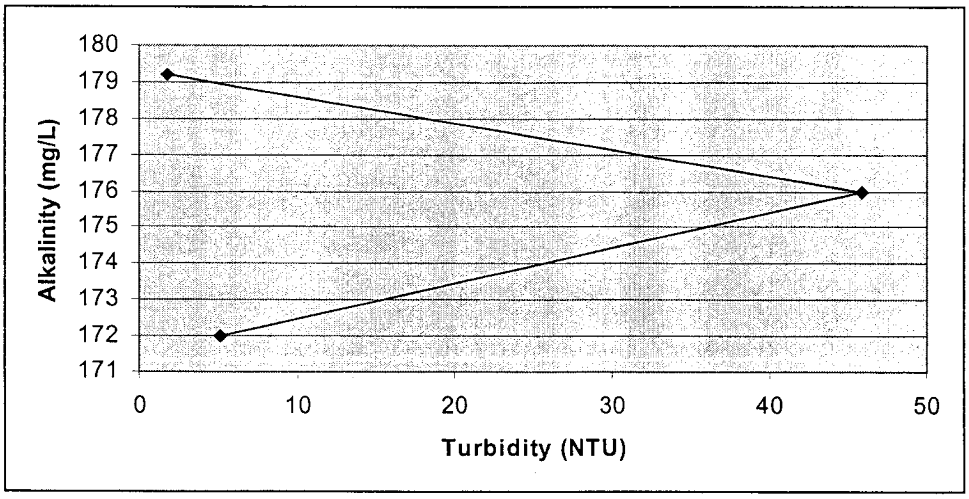

Figure 4-14 Relationship between turbidity and Alkalinity in medium pressure UV systems

No conclusions can be drawn from this figure. Moreover, other relationships, such as Turbidity vs. TOC or Hardness, Alkalinity vs. TOC or Hardness, and TOC vs. Hardness, also show similar patterns to the above. Hence, the combination could not be realised. The main reason is the lack of data, because only three data points in each of two correlated variables can be used to determine any of the relationships.

The relationship between wastewater quality (as represented by Turbidity, TOC, Hardness and Alkalinity) and SUVT (being the combination of SUVT, fouling rates and roughness) cannot be decided either, because any parameter describing wastewater quality shows a similarly irregular relationship to SUVT. For instance, Figure 4-15 shows the relationship between SUVT and Turbidity.

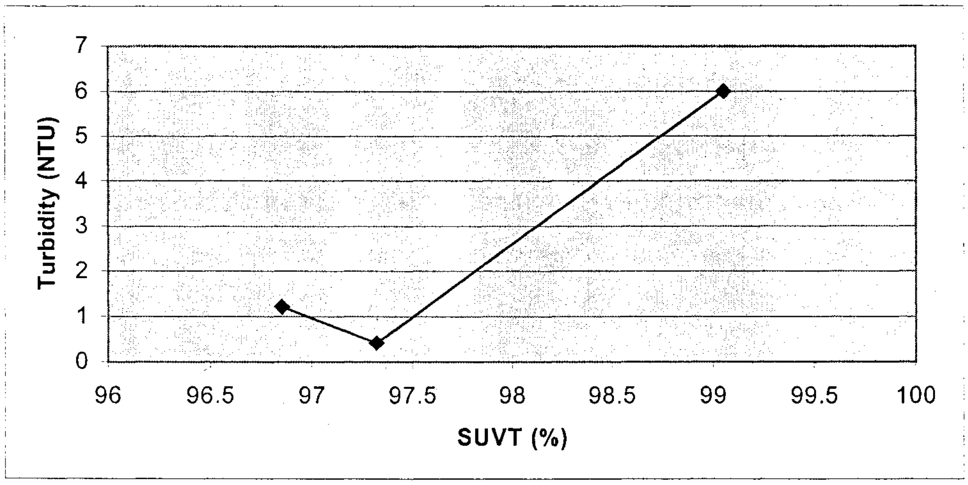

Figure 4-15 Relationship between SUVT and turbidity in medium pressure UV systems

Overall, the analysis shows that wastewater quality can affect permanent fouling to some extent, but the relationship found in this research is not very robust.

In this study, the major factor causing permanent fouling appeared to be physical damage of the sleeves (i.e. scratching) rather than wastewater quality. Mechanical deterioration is initiated and aggravated by mechanical cleaning in mechanical or chemical/mechanical cleaning systems. Therefore, the main method for attenuating the affects of the permanent foulants should be to renovate chemical/mechanical cleaning systems at specific sites.

4.6 Removing "Permanent" Foulants

Since physical damage of the sleeves and accumulation of permanent foulants cannot be avoided altogether, the only way for lessening the impacts of permanent foulants is to remove them by chemicals which are used for chemical cleaning.

Three chemical solutions were chosen for removing the permanent foulants on the sleeve samples whose SUVT was below 98%. The selected samples were C1, D1, Y, and S. The three chemical solutions were 0.2% sodium hydroxide, 0.15% sodium bisulfite (Kreft et al., 1986), and 85% phosphoric acid. The effect of removing the permanent foulants was measured by changes of the SUVT.

Each sample was divided into three parts, which were immersed in these three solutions respectively. After 1, 2, 3, 4, 8, 10, 24, and 48 hours, they were removed, washed by distilled water and dried by lint free paper, then their SUVT was measured. In general, after 10 hours, their UV transmittance had not changed. After 24 hours, the changes of SUVT were relatively obvious. 48 hours later, their SUVT was similar to that after 24 hours. Thus, only the SUVT that was measured after 24 hours is compared here. Tables 4-11 to 4-14 show the SUVT values for the different samples.

Table 4-11 SUVT of Sample C1 after three immersions

Samples	SUVT
Sample C1 before immersion	0.97
Part of C1 after NaOH	0.9788
Part of C1 after $NaHSO_3$	0.9812
Part of C1 after H_3PO_4	0.9775

From Table 4-11, it is seen that the SUVT of the three parts of Sample C1 after the different immersions is only slightly higher than that before the immersions, which proves that these three solutions were effective to some extent. Although the SUVT of the part immersed in sodium bisulfite exceeded 98%, the difference between it and the other two parts was too small to claim that the sodium bisulfite was more useful for removing the permanent foulants on Sample C1.

Table 4-12 SUVT of Sample D1 after three immersions

Samples	SUVT
Sample D1 before immersion	0.97
Part of D1 after NaOH	0.9952
Part of D1 after $NaHSO_3$	0.9878
Part of D1 after H_3PO_4	0.9966

From Table 4-12, it is seen that these three solutions were all effective in the removal of permanent foulants from Sample D1. 85% phosphoric acid was more suitable for the application because it was cheaper than sodium hydroxide but had the same behavior. In fact, phosphoric acid was already used in System D, but Sample D1 had only a relatively low SUVT. This contrasting behaviour may be attributed to a cleaning system which did not allow the phosphoric acid to stay on the sleeves long enough to remove most of foulants.

Table 4-13 SUVT of Sample Y after three immersions

Samples	SUVT
Sample Y before immersion	0.977
Part of Y after NaOH	0.99
Part of Y after $NaHSO_3$	0.979
Part of Y after H_3PO_4	0.976

From Table 4-13, it is obvious that sodium hydroxide was the most suitable chemical for removing the permanent foulants on Sample Y. Perhaps sodium hydroxide should take the place of phosphoric acid in System Y if the costs are not significantly different.

Table 4-14 SUVT of Sample S after three immersions

Samples	SUVT
Sample S before immersion	0.94
Sample S after NaOH	0.93
Sample S after $NaHSO_3$	0.93
Sample S after H_3PO_4	0.9988

Phosphoric acid was effective in removing the permanent foulants from Sample S. However, System S had already been applying phosphoric acid for the chemical/mechanical cleaning, yet Sample S had only a moderate SUVT. This could be because the concentration of the phosphoric acid applied in System S was much lower, the interval between cleanings was too long, and/or the cleaning period was too short.

In general, to remove permanent foulants from the sleeves of UV systems, the most suitable chemicals should be chosen by tests similar to those reported herein, as well as pilot operations. Sodium hydroxide, sodium bisulfite and phosphoric acid could be suitable candidates. A shortcoming of the batch tests is obviously that the sleeves in the real operations cannot be immersed in the chemicals for periods similar to those used in the laboratory. Nevertheless it may be prudent on, say, an annual basis, to "revive" sleeves by immersing them for an extended time, as a batch operation, in the cleaning solutions.

Chapter 5 Conclusions and Recommendations

5.1 Conclusions

This research showed that chemical/mechanical cleaning was more effective in removing foulants on sleeves covering UV lamps than mechanical cleaning alone. The intervals of chemical/mechanical cleaning were dictated by site specific fouling rates. Although chemical/mechanical cleaning was effective, permanent foulants that could not be removed completely always remained on the sleeves. These permanent foulants reduce UV transmittance of the sleeves; as a result, sleeves after a certain period of service cannot regain 100% UV transmittance.

The findings in this research indicated that permanent foulants were trapped initially by the inherent holes and peaks on sleeve surfaces. After periodical chemical/mechanical cleaning, the wipers of cleaning systems can damage sleeve surfaces, causing scratches or holes of significant surface areas, which is referred to herein as mechanical deterioration of the sleeves. Thus, foulants can be trapped more easily by these scratches and holes, and adhere tightly to the surfaces of these scratches or to each other. These foulants can contribute to permanent fouling, which was shown by the increased roughness of sleeve surfaces and the decreased UV transmittance. This implies that the mechanical cleaning in chemical/mechanical cleaning systems increases permanent fouling and cannot be avoided.

Mechanical damage of the surfaces of the sleeves undergoing chemical/mechanical cleaning appears to be less than that on the sleeves experiencing only mechanical cleaning. This could be due to the longer intervals for chemical/mechanical cleaning than those for mechanical cleaning, and/or that if mechanical cleaning is used alone, it needs to be harsher than if it is combined with chemical cleaning.

Chemical analyses showed that the compositions of these permanent foulants varied for each plant, and were site specific. In general, iron, aluminum, calcium, magnesium and phosphorus composed the majority of the mass of the materials in the permanent foulants.

An attempt was made to correlate the nature of the permanent foulant to the site specific wastewater quality. However, although it was shown that wastewater quality can affect permanent fouling to some extent, for example, that poor wastewater quality was more likely to cause the permanent fouling, there was no robust statistical relationship between them, especially for sleeves from low pressure UV systems. Thus specific wastewater quality parameters cannot at this stage predict the future influence of that wastewater on permanent fouling.

An important factor causing permanent fouling is mechanical deterioration of sleeves, rather than wastewater quality. Mechanical deterioration was initiated and aggravated by the mechanical cleaning component of the chemical/mechanical cleaning systems, which basically cannot be avoided altogether. Therefore, the main method for diminishing the affect of permanent foulants should be to renovate chemical/mechanical cleaning systems at specific sites, such as by choosing the most suitable cleaning chemicals which can remove the majority of permanent foulants or by adjusting the structure or operation of chemical/mechanical cleaning systems so that the mechanical damage can be lessened.

It is generally impractical to substantially modify existing cleaning systems, so the practical way for removing permanent foulants and for reducing their buildup is to choose the most suitable cleaning chemicals, which should be determined by laboratory experiments and pilot operations. Sodium hydroxide, sodium bisulfite and phosphoric acid appear to be appropriate candidates. Certainly, economical factors should also be considered.

5.2 Recommendations

The most suitable cleaning chemicals should be decided at specific sites, hence pilot operations are needed. Since chemical immersion is usually not possible for the sleeves in real operations, the concentration and formulation of cleaning chemicals which were optimized by laboratory experiments, need to be verified by pilot operations.

Moreover, for chemical/mechanical cleaning systems, which can cause mechanical damage to sleeves, renovation may be necessary. With the precondition of keeping satisfactory SUVT and disinfecting effectiveness of UV systems, the frequency of cleaning should be decreased to minimize mechanical damage. Softer mechanical wipers could also be employed to reduce mechanical damage. Finally, to ensure that all parts of the sleeves can be cleaned to a similar extent, (which would avoid different levels of permanent fouling at different parts of the sleeves, such as that found for Samples X1 and X2), cleaning systems may need to be adjusted to achieve this aim.

In this research, the mathematical correlations developed between wastewater quality and permanent fouling were not robust because of the lack of data for wastewater quality. For example, in the four low pressure UV systems, a specific parameter of wastewater quality was measured in three systems but was absent in the fourth. For further research, to determine the influence of wastewater quality on permanent fouling at specific sites, more data for wastewater quality and permanent fouling are needed.

References

Angehrn, M. (1984) *Ultraviolet disinfection of water.* J. Wat. SRT-Aqua, 2, 109-115

Aquionics Inc. (2002) *Ultraviolet technology update.* Retrieved from http://www.aquionics.com/UVtechupdate.htm.

Banwart, S.A. (1999) *Reduction of iron (III) minerals by natural organic matter in groundwater.* Geochimica and Cosmochimica Acta, Vol. 63, No. 19/20, 2919-2928.

Benefield, L.D., Judkins, J.F. and Weand, B.L. (1982) *Process chemistry for water and wastewater treatment.* Prentice-Hall, Inc. New Jersey, USA.

Black, S., Serworks, C., Yust, L., and Curtis, T. (1993*) Application of UV disinfection at the Georgetown WPCP.* Proc. "Planning, design & operation of effluent disinfection systems", Water Environment Federation Specialty Conf., Whippany, NJ.

Blatchley, E.R. (1997) *Ultraviolet disinfection: process characteristics and modelling.* "Wastewater disinfection: chlorine vs. UV light. What is the truth?" WEFTEC 70th annual conference, Water Environment Federation, Chicago, IL, USA.

Blatchley, E., Bastian, K., Duggirala, R., Hunt, B., Alleman, J., Wood W., Moore M., Anderson, B., and Schuerch P. (1993) *Large scale pilot investigation of ultraviolet disinfection.* Proc. "Planning, design & operation of effluent disinfection systems", Water Environment Federation Specialty Conf., Whippany, NJ.

Blatchley, E.R.III, Bastian, K.C., Duggirala, R.K., Alleman, J.E., Moore, M. and Schuerch, P. (1996) *Ultraviolet irradiation and chlorination/dechlorination for municipal wastewater disinfection: assessment of performance limitations.* Water Environment Research, Vol. 68, No. 2, 194-204.

Bolton, J.R. (1999) *Ultraviolet applications handbook.* Bolton Photoscience Inc. Edmonton, AB, Canada.

Bott, T.R. (1995) *Fouling of heat exchangers.* Elsevier, Amsterdam, NY, USA.

Cairns, W. (1996) *Comparison of UV disinfection technologies using low intensity monochromatic and high intensity polychromatic UV lamps.* Proc. "Disinfecting Wastewater for Discharge and Reuse", Water Environment Federation, Portland, OR, March 17-20.

Cairns, W.L. and McKee, J. (1996) *New advances in ultraviolet light disinfection technology.* Water Environment Association of Ontario Technical Symposium Toronto, Ontario, March 24-26.

Chinniah, K. and Kwan, A. (1996). *Performance standards and design guidelines for effluent disinfection in Alberta.* Proc. "Disinfecting Wastewater for Discharge and Reuse", Water Environment Federation, Portland, OR, March 17-20.

Correia, C. and Snider, K. (1993) *Pilot-scale evaluation of UV disinfection at treatment facilities in the state of Oregon.* Proc. "Planning, design & operation of effluent disinfection systems ", Water Environment Federation Specialty Conf., Whippany, NJ.

Diamant, B.Z. (1996) *Water treatment: the ultraviolet option.* Water Irrig. Rev. 16 (3), 24-30.

Digital Instruments (di), (1998) *NanoScope command reference manual.* Santa Barbara, CA, USA.

Fukushima, M. and Tatsumi, K. (1999) *Light acceleration of iron (III) reduction by humic acid in the aqueous solution.* Colloids and Surfaces A: Physicochemical and Engineering Aspects, Vol. 155, 249-258.

Gabriel, B.L. (1985) *SEM : a user's manual for materials science.* American Society for Metals, Metals Park, OH, USA.

Gaylarde, C and Videla, H. (1995) *Bioextraction and biodeterioration of metals.* Cambridge University Press, Cambridge, U.K.

Geesey, G., Lewandowski, Z., and Flemming, H. (1993) *Biofouling and biocorrosion in industrial water systems.* Lewis Publishers, USA.

Gehr, R., Comair, C. B. and Cairns, W.L. (1993) *UV disinfection of wastewater by medium-pressure lamps.* Proc. Joint CSCE/ASCE National Conference on Environmental Engineering, Montreal, July 12-14.

Gehr, R. and Wright, H. (1998) *UV disinfection of wastewater coagulated with ferric chloride: recalcitrance and fouling problems.* Wat. Sci. Tech. Vol. 38 (3), 15-23.

Howland, R. and Benatar, L. (1996) *A practical guide to the scanning probe microscope.* Park Scientific Instruments, Sunnyvale, CA, USA.

James, D., Truong, M., Amy, P., Steubing, P., Lagadinos, T., Igbinovia, A., Shumaker, S., Bain, R., Soroushian, F., Award, J. and Whitby, G.E. (1996) *UV disinfection of effluent treated with lime or ferric chloride coagulants.* Proc. "Disinfecting Wastewater for Discharge and Reuse", Water Environment Federation, Portland, OR, March 17-20.

Jesien, W. (1998) *Fouling of UV lamps during disinfection in pilot plant and full-scale applications.* M. Eng. Project Report. Dept. of Civil Engineering and Applied Mechanics, McGill University, Montreal, QC, Canada.

Job, G.D., Trengove, R. and Realey, G.J. (1995) *Trials using a mobile ultraviolet disinfection system in South West Water.* J. CIWEM, Vol. 9, No. 6, 257-263.

JEOL USA, Inc (2002).
Retrieved from http://www.jeol.com/sem_gde/distort.html

Kreft, P., Scheible, O.K., and Venosa, A. (1986) *Hydraulic studies and cleaning evaluations in ultraviolet disinfection units.* Water Pollution Control Federation Journal Vol. 58, No. 12, 1129-1137.

Lin, L. (2000) *Numerical modelling of inorganic fouling processes.* Retrieved from http://ce.ecn.purdue.edu/~lianshin/modelling.html.

Lin, L., Johnston, C.T., and Blatchley, E. (1997) *Mechanism of inorganic fouling at quartz:water interfaces in ultraviolet photoreactors.* Water Environment Federation 70th annual conference & exposition 1, 277-287.

Lin, L., Johnston, C.T. and Blatchley, E.R.III (1999a) *Inorganic fouling at quartz:water interfaces in ultraviolet photoreactors- I. chemical characterisation.* Water Research, Vol. 33, No. 15, 3321-3329.

Lin, L., Johnston, C.T. and Blatchley, E.R.III (1999b) *Inorganic fouling at quartz:water interfaces in ultraviolet photoreactors- II. temporal and spatial distribution.* Water Research, Vol. 33, No. 15, 3330-3338.

Mishalani, N.R., Koester, P.A., and Thyamagondalu, P. (1996) *Effect of water quality on UV transmittance: the Burbank case study.* Proc. "Disinfecting Wastewater for Discharge and Reuse", Water Environment Federation, Portland, OR, March 17-20.

Muller, S. (2000) *Handbook of heat exchanger fouling : mitigation and cleaning technologies.* Essen : Publico Publications, Rugby, U.K.

O'Brien, W.J., Hunter, G.L., Rosson, J.J., Hulsey, R.A. and Carns, K.E. (1996) *Ultraviolet system design: past, present, and future.* Proc. "Disinfecting Wastewater for Discharge and Reuse", Water Environment Federation, Portland, OR, March 17-20.

Ohio Pure Water Company. (2002) *The advantages of UV disinfection.* Retrieved from http://www.ohio-water-purifiers.com/ultraviolet-disinfection.html.

Oliver, M. (2002) *Validation of cleaning methods for UV disinfection systems.* Proc. "Disinfection 2002", Water Environment Federation Specialty Conf. St. Petersburg, Feb. 17-20.

Ontario Centre for Environmental Technology Advancement (2002) Retrieved from http://www.oceta.on.ca/profiles/catalogue.html.

Pinto, D., and Santamaria, M. (1999) *Characterization of fouling of UV disinfection lamps in the absence and presence of ferric chloride coagulant.* M. Eng. Project Report. Dept. of Civil Engineering and Applied Mechanics, McGill University, Montreal, QC, Canada.

Qiu, Y. (2001) *Characterisation of the surface of quartz sleeves surrounding UV disinfection lamps*. M. Eng. Project Report. Dept. of Civil Engineering and Applied Mechanics, McGill University, Montreal, QC, Canada.

Ramos, B. (2001) *Investigation of fouling of quartz sleeves using a laboratory scale UV disinfection system.* M. Eng. Project Report. Dept. of Civil Engineering and Applied Mechanics, McGill University, Montreal, QC, Canada.

Rose, J., Vilge, A., Olivie-Lauquet, G., Masion, A., Frechou, C., and Botterom, J.Y. (1998) *Iron speciation in natural organic matter colloids.* Colloids and Surfaces A: Physicochemical and Engineering Aspects, Vol. 136, 11-19.

Royal Philips Electronics Inc. (2002)
Retrieved from http://www.panalytical.com/technologies/xrf.

Sedlack, R. (1991) *Phosphorous and nitrogen removal from municipal wastewater: principles and practice.* 2nd ed. Lewis Publishers, Chelsea, MI.

Sehnaoui, K. (2001) *Fouling of UV lamp sleeves: exploring inconsistencies in the role of iron.* M. Eng. Thesis Report. Dept. of Civil Engineering and Applied Mechanics, McGill University, Montreal, QC, Canada.

Sheriff, M. (1999) *Laboratory investigation of inorganic fouling of UV disinfection lamps.* M. Eng. Project Report. Dept. of Civil Engineering and Applied Mechanics, McGill University, Montreal, QC, Canada.

Sheriff, M. and Gehr, R. (2001) *Laboratory investigation of inorganic fouling of low pressure UV disinfection lamps.* Water Quality Research Journal Canada, Vol. 36, No. 1, 71-92.

Snoeyink, V.L. and Jenkins, D. (1980) *Water Chemistry.* John Wiley and Sons, NY, USA.

Soroushian, F., Noesen, M., Jaques, R., and Tchobanoglous, G. (1996) *Impact of chemicals on reclaimed water disinfection.* Proc. “Planning, design & operation of effluent disinfection systems”, Water Environment Federation Specialty Conf., Whippany, NJ, 1996.

Stumm, W. (1992) *Chemistry of the solid:water interface.* John Wiley & Sons Inc., NY, USA.

Temmer, B., Soroushian, F., and Noesen, M. (2000) *UV emerges as bright spot for wastewater disinfection*. Pollution Engineering Online. Retrieved from http://www.pollutionengineering.com/archives/2000/pol0901.00/pol0900F2.htm.

Topnik, J.M., Smith, D.W., and Buchanan, I.D. (2000) Iron in Wastewater: Effect on Quartz Sleeve Scale. WEFTEC North America 2000, Anaheim, CA, USA.

Trojan Technologies Inc. (2002) Retrieved from http://www.trojanuv.com.

University of Nebraska at Lincoln. (2002)
Retrieved from http://www.unl.edu/CMRAcfem

USEPA. (1986) *Design manual: municipal wastewater disinfection.* EPA/625/1-86/021. Cincinnati, OH, US Environmental Protection Agency, Washington, DC.

USEPA. (2002) *Ultraviolet Disinfection.* No. CX824652. Cincinnati, OH, US Environmental Protection Agency, Washington, DC.

WEF. (1996) *Wastewater disinfection.* Water Environment Federation, Alexandria, VA, USA.

Appendix A

Questionnaire for Information Collection

Page 1

Date:

Name of plant:

Operator:

Address:

Telephone:
Fax:
Email:

Average daily flow				
Upstream processes (please list them in sequence used)				
Chemicals used and dose (for sedimentation, disinfection, coagulation, and so on)	Name	Dose	Name	Dose
Average wastewater quality (if possible, please indicate summer or winter)	pH		BOD	
	COD		SS	
	Turbidity		Alkalinity	
	Temperature		TOC	
	Main inorganics, organics and metal ions			
	Name	Concentration	Name	Concentration

Page 2 **Date:**

Average wastewater quality (if possible, please indicate summer Or winter)	Main inorganics, organics and metal ions (continue)			
	Name	Concentration	Name	Concentration
UV system details	Manufacturer			
	Date installed			
	Type of UV lamp (low pressure or medium pressure)			
	Age of sleeves			
	Fouling measurement method			
	Cleaning method (chemicals included or not, if possible, please indicate clearly)			
	Frequency of cleaning			
	Maintenance period after cleaning			
	Transmittance before cleaning			
	Transmittance after cleaning			

Appendix B

Raw Data from XRF Analyses

Geochemical Laboratories
Earth and Planetary Sciences
McGill University, 3450 University Street
Montreal, QC   CANADA   H3A 2A7

Major Element Package

No.			SiO2	Al2O3	Fe2O3	MgO	CaO	Na2O	K2O	P2O5	BaO	Cr2O3	Cl	SO3	C
PENG02	**013**	**CONTROL**	99.92	0.01		0.02	0.03							0.01	
PENG02	**012**	**A**	99.90	0.03	0.01	0.02	0.02								
PENG02	**009**	**B1**	99.88	0.01		0.02	0.02			0.04					
PENG02	**010**	**B2**	90.57	0.45	0.25	0.37	0.71	0.01		6.16			0.09	0.22	1.10
PENG02	**011**	**B3**	90.30	0.49	0.26	0.39	0.70	0.07		6.29			0.03	0.18	1.27
PENG02	**006**	**C1**	99.87		0.04	0.02	0.01			0.02		0.02			
PENG02	**007**	**C2**	99.19	0.06	0.05	0.04	0.08	0.02		0.48		0.01	0.02	0.04	
PENG02	**008**	**C3**	89.58	0.37	0.61	0.19	0.65	0.08	0.01	6.43			0.03	0.22	1.82
PENG02	**004**	**D1**	99.84	0.01		0.02	0.06			0.03				0.02	
PENG02	**005**	**D2**	97.71	0.22	0.09	0.09	0.15	0.07		1.57			0.02	0.07	
PENG02	**003**	**D3**	87.98	1.26	0.54	0.24	0.76	0.07		7.57	0.01		0.05	0.28	1.23
Detection Limits (%):			**0.01**	**0.01**	**0.01**	**0.01**	**0.01**	**0.01**	**0.01**	**0.01**	**0.01**	**0.01**	**0.01**	**0.01**	**0.01**

Note: The results are expressed as weight percent.
Analyses done on samples as received.
Detection limits are based on three times the background sigma values.

August 9, 2002

Geochemical Laboratories
Earth and Planetary Sciences
McGill University, 3450 University Street
Montreal, QC CANADA H3A 2A7

Major Element Package

No.			SiO2	Al2O3	Fe2O3	MgO	CaO	Na2O	P2O5	Cr2O3	Cl	F	SO3	C
PENG02	**014**	**NEW**	99.97			0.02								
PENG02	**015**	**X (yellow)**	78.30	5.81	0.47	0.24	0.58	0.04	12.52	0.02	0.01		0.06	1.93
PENG02	**016**	**X (clear)**	99.91		0.04	0.02				0.02				
PENG02	**017**	**Y**	91.99	1.97	0.08	0.09	0.20	0.08	3.93	0.02	0.01	0.27		1.35
PENG02	**018**	**Z**	99.43											0.56
Detection Limits(%):			**0.01**	**0.01**	**0.01**	**0.01**	**0.01**	**0.01**	**0.01**	**0.01**	**0.01**	**0.01**	**0.01**	**0.01**

Note: The results are expressed as weight percent.
Analyses done on samples as received.
Detection limits are based on three times the background sigma values.

September 9, 2002